



1 **Surface water and groundwater: Unifying**
2 **conceptualization and quantification of the two “water**
3 **worlds”**

4
5
6 Brian Berkowitz¹, Erwin Zehe²

7
8 1. Department of Earth and Planetary Sciences, Weizmann Institute of Science, Rehovot
9 7610001, Israel

10 2. Karlsruhe Institute of Technology (KIT), Karlsruhe, Germany

11
12 *Correspondence to:* Brian Berkowitz (brian.berkowitz@weizmann.ac.il)

13
14
15 **Abstract.**

16
17 While both surface water and groundwater hydrological systems exhibit structural, hydraulic
18 and chemical heterogeneity, and signatures of self-organisation, modelling approaches
19 between these two “water world” communities generally remain separate and distinct. To
20 begin to unify these water worlds, we recognize that preferential flows, in a general sense, are
21 a manifestation of self-organisation; they hinder perfect mixing within a system, due to a
22 more “energy efficient” and hence faster throughput of water and matter. We develop this
23 general notion by detailing the role of preferential flow for residence times and chemical
24 transport, as well as for energy conversions and energy dissipation associated with flows of
25 water and mass. Our principal focus is on the role of heterogeneity and preferential flow and
26 transport of water and chemical species. We propose, essentially, that related
27 conceptualizations and quantitative characterisations can be unified in terms of a theory that
28 connects these two water worlds in a dynamic framework. We discuss key features of fluid
29 flow and chemical transport dynamics in these two systems – surface water and groundwater
30 – and then focus on chemical transport, merging treatment of many of these dynamics in a
31 proposed quantitative framework. We then discuss aspects of a unified treatment of surface
32 water and groundwater systems in terms of energy and mass flows, and close with a reflection
33 on complementary manifestations of self-organisation in spatial patterns and temporal
34 dynamic behaviour.

35
36
37
38 **Keywords:** Chemical transport, Continuous Time Random Walk (CTRW), self-organisation,
39 preferential flow



40 1 INTRODUCTION

41 While surface and subsurface flow and transport of water and chemicals are strongly
42 interrelated, the respective communities are split into two “water worlds”. The communities
43 even separate terminology, writing “surface water” as two words but “groundwater” as one
44 word!

45 At a very general level, it is well recognized that both surface water and groundwater
46 systems exhibit enormous structural and functional heterogeneity, which are, e.g., manifested
47 through the emergence of preferential flow and space-time distributions of water, chemicals,
48 sediments and colloids, and energy across all scales and within/across compartments (soil,
49 aquifers, surface rills and river networks, full catchment systems, and vegetation). Dooge
50 (1986) was among the first hydrologists who distinguished between different types of
51 heterogeneity – namely, between stochastic and organised/structured variability – and
52 reflected upon how these forms affect predictability of hydrological dynamics. He concluded
53 that most hydrological systems fall into Weinberg’s (1975) category of organised complexity
54 – meaning that they are too heterogeneous to allow pure deterministic handling but exhibit too
55 much organisation to enable pure statistical treatment.

56 A common way to define spatial organisation of a physical system is through its distance
57 from the maximum entropy state (Kondepudi and Prigogine, 1998; Kleidon, 2012). Isolated
58 systems, which do not exchange energy, mass, or entropy with their environment, evolve due
59 to the second law of thermodynamics to a perfectly mixed “dead state” called thermodynamic
60 equilibrium. In such cases, entropy is maximized and Gibbs free energy is minimized,
61 because all gradients have been dissipated by irreversible processes. Hydrological systems
62 are, however, open systems, as they exchange mass (water, chemicals, sediments, colloids),
63 energy and entropy across their system boundaries with their environment. Hydrological
64 systems may hence persist in a state far from thermodynamic equilibrium. They may even
65 evolve to states of a lower entropy, and thus stronger spatial organisation, for instance through
66 steepening of gradients, for example, in topography, or in the emergence of structured
67 variability of system characteristics or network-like structures. Such a development is referred
68 to as “self-organisation” (Haken, 1983) because local scale dissipative interactions, which are
69 irreversible and produce entropy, lead to ordered states or dynamic behaviours at the (macro-)
70 scale of the entire system. Self-organisation requires free energy transfer into the system to
71 perform the necessary physical work, self-reinforcement through a positive feedback to assure
72 “growth” of the organised structure/patterns in space, and the export of the entropy which is
73 produced within the local interactions to the environment (Kleidon, 2012).

74 Manifestations of self-organisation in *surface water systems* are manifold. The most
75 obvious one is the persistence of smooth topographic gradients (Reinhardt and Ellis, 2015;
76 Kleidon et al. 2012), which reflect the interplay of tectonic uplift and the amount of work
77 water and biota have performed to weather and erode solid materials, to form soils and create
78 flow paths. Although these processes are dissipative and produce entropy, they nevertheless
79 leave signatures of self-organisation in catchment systems. These are expressed, for instance,
80 through the soil catena – a largely deterministic arrangement of soil types along the
81 topographic gradient of hillslopes (Milne, 1931; Zehe et al., 2014) – and even more strongly
82 through the formation of rill and river networks (Fig. 1) at the hillslope and catchment scales



83 (Howard, 1990; Paik and Kumar, 2010; Kleidon et al., 2013). These networks form because
84 flow in rills is, in comparison to sheet flow, associated with a larger hydraulic radius, which
85 implies less frictional energy dissipation per unit volume of flow. This causes higher flow
86 rates, which in turn may erode more sediment. As a result, these networks commonly increase
87 the efficiency in transporting water, chemicals, sediments and energy through hydrological
88 systems, which results also in increased kinetic energy transport through the network and
89 across system boundaries.

90 In contrast, the term self-organisation is rarely applied to *groundwater systems*, except in
91 the context of positive/negative feedbacks during processes of precipitation and dissolution
92 (e.g., Worthington and Ford, 2009). We argue, though, that the subsurface, too, displays some
93 characteristics of (partial) self-organisation. This is manifested, in particular, through
94 ubiquitous, spatially correlated, anisotropic patterns of soil or aquifer (structural, hydraulic)
95 properties, particularly in non-Gaussian systems (Bardossy, 2006), as these have much
96 smaller entropy compared to uncorrelated noise patterns. The emergence and persistence of
97 preferential pathways even in homogeneous sand packs (e.g., Hoffman et al., 1996; Oswald et
98 al., 1997; Levy and Berkowitz, 2003) is a striking example of formation of a self-organised
99 pattern of “smooth fluid pressure gradients”.

100



101

102 **Figure 1** Hillslope scale rill networks developed during an overland flow event at the
103 Dornbirner Ach Austria (left panel, we gratefully acknowledge the Copyright holder © Ulrike
104 Scherer KIT) and the South Fork of Walker Creek in California (right panel, we gratefully
105 acknowledge the Copyright holder © James Kirchner ETH Zürich)

106

107 Our general recognition is that hydrological systems exhibit – below and above ground –
108 both (structural, hydraulic and chemical) heterogeneity and signatures of (self-)organisation.
109 We propose that all kinds of preferential flow paths/flow networks veining the land surface
110 and the subsurface are prime examples of spatial organisation (Bejan et al., 2008; Rodriguez-
111 Iturbe and Rinaldo, 2001) because they exhibit, independently of their genesis, similar
112 topological characteristics. Our starting point to unify both water worlds is the recognition
113 that any form of preferential flow is a manifestation of self-organisation, because it hinders
114 perfect mixing within a system and implies a more “energy efficient” and hence faster
115 throughput of water and matter (Rodriguez-Iturbe et al., 1999; Zehe et al., 2010; Kleidon et
116 al., 2013). This general notion can be elaborated further by detailing the role of preferential



117 flow for residence times and transport of chemical species as well as for energy conversions
118 and energy dissipation associated with flows of water and mass.

119 The main focus of this contribution is on the role of heterogeneity and preferential flow
120 and transport of water and chemical species. We propose, essentially, that related
121 conceptualizations and quantitative characterizations can be unified in terms of a theory that
122 connects these two water worlds in a dynamic framework. We first discuss key features of
123 fluid flow and chemical transport dynamics in these two systems – surface water and
124 groundwater – using the (often distinct) terminology of each of these “water world” research
125 communities. We outline the particular questions, methods, limitations, and uncertainties in
126 each “world” (Section 2). We then focus on chemical transport, merging treatment of many of
127 these dynamics in a proposed quantitative framework, and providing specific examples
128 (Section 3). In Section 4, we briefly discuss aspects of a unified treatment of surface water
129 and groundwater systems in terms of energy and information flows. Final conclusions and
130 perspectives appear in Section 5.

131 **2 TWO WATER WORLDS – UNIQUE, DIFFERENT AND SIMILAR**

132 In both worlds, a major focus is on travel times and residence times of water, as they
133 provide the main link between water quantity and quality. Surface water deals also with
134 extremes, i.e., floods and droughts as well as land surface-atmosphere feedbacks, fluvial
135 geomorphology and eco-hydrology.

136 From the outset, we recognise that flow in both surface water and groundwater systems is
137 controlled by the interplay of potential energy differences, usually expressed as potential
138 gradients, and frictional losses, which dissipate a substantial part of the driving energy
139 difference along the flow path into heat. Overland and channel flows are driven by
140 topography – gravitational potential energy differences – and it is well known that only a tiny
141 amount of the driving energy difference is converted into kinetic energy of overland or
142 channel flow (Loritz et al., 2019), while more than 99% is dissipated along the hillslope or in
143 the channel. Frictional losses are essentially turbulent, thus proportional to the square of the
144 fluid velocity, and occur mainly at the contact line between the fluid and the solid (the land
145 surface or the wetted perimeter of the rill or the channel cross section), while internal fluid
146 friction is small. This “weak interaction” between fluid and solid is, according to Kleidon et
147 al. (2013), *the* reason why a wider channel/rill cross-section leads, due to the larger hydraulic
148 radius, to a smaller frictional loss per unit volume of flow and a more energy efficient
149 transport.

150 Flow through subsurface porous media is driven by gradients in total hydraulic potentials,
151 reflecting differences in gravitational potential, matric potential and pressure potential
152 energies. Flow is essentially laminar and frictional losses grow linearly with fluid velocity.
153 Despite the fact that the driving gradients are at least in the vadose zone frequently larger than
154 1 m m^{-1} , implying accelerations larger than Earth’s gravitational acceleration g (m s^{-2}), flow
155 velocities are several orders of magnitude smaller than in surface water systems. Kinetic
156 energy in subsurface matrix flow is thus practically zero, reflecting the much higher frictional
157 dissipation, due to strong interaction of the fluid with the usually very large specific surface of
158 the pore space. Flow within subsurface preferential pathways (macropores, fractures) is,



159 however, characterised by (relatively weak interaction between fluid and solid, similar to flow
160 in rills or river networks. This implies a reduced frictional loss, higher flow velocities (and
161 kinetic energy), and rapid transport and imperfect mixing of chemicals. As such, the Darcy-
162 Buckingham law is inappropriate to characterize preferential flow (Beven and Germann,
163 1982, 2013), as detailed further in Sects. 2.1 and 2.2.

164 The generally much slower fluid velocities in groundwater systems do not, however,
165 imply slow hydraulic response times during rainstorms; on the contrary, aquifers may release
166 almost instantaneously older, pre-event water into a catchment outlet stream. This apparent
167 paradox – referred to by some researchers as the “old-new water paradox” (Kirchner, 2003) –
168 is explained by propagation of pressure waves. Shear or compression waves (or waves in
169 general) transport momentum and energy through continua *without an associated transport of*
170 *mass or particles* (Everett, 2013; Goldstein, 2013); and their speed (or “celerity”; see Sect. 3.1
171 for discussion) is many orders of magnitude larger than the fluid velocity in aquifer systems
172 (McDonnell and Beven, 2014).

173 Although these interactions and phenomena are well known, we emphasise them as they
174 highlight why one cannot separate a river from its catchment, nor the land surface from the
175 underlying soil-aquifer system. Stream flow response to rainfall is composed of “waters of
176 different ages”, reflecting overland flow, subsurface storm flow and base-flow contributions
177 with their specific, usually non-Gaussian travel time distributions and chemical signatures.
178 Depending on landscape setting and the dominant runoff mechanisms, pre-event water
179 fractions in storm runoff reach from near zero to more than 60% of storm water having an
180 isotopic signature different from that of rainfall (Sklash and Farvolden, 1979; Sklash et al.,
181 1996; Blume et al., 2008).

182 In the following, we elaborate briefly on the specific model paradigms in surface water,
183 soil and groundwater water systems with an emphasis on preferential pathways for fluid flow
184 and chemical transport, and on the resulting ubiquitous, anomalous early and late time arrivals
185 of chemicals to measurement outlets.

186 **2.1 Surface water systems and catchment hydrology**

187 Catchment hydrology developed largely as an engineering discipline around traditional
188 tasks of designing and operating reservoirs, flood risk assessment and water resources
189 management (Sivapalan, 2018). These “bread and butter” tasks require successful predictions
190 of stream flow response at the catchment outlet (Sivapalan, 2018), which may be achieved
191 with conceptual bucket models such as the well-known HBV model (Lindstrom et al., 1997).
192 Due to their mathematical simplicity, these conceptual models are straightforward to code
193 (particularly in modern scripting languages); moreover, the advent of combinatorial
194 optimization methods for automated parameter search, and fast computers (Duan et al., 1992;
195 Bardossy and Singh, 2008; Vrugt and Ter Braak, 2011) have also made their calibration and
196 validation a straightforward venture. As a consequence, these conceptual models gained
197 enormous popularity in catchment hydrology, and despite their well-known equifinality –
198 meaning that several model structures usually fit the target data equally well (Beven and
199 Binley, 1992) – they are, to date, the first choice for predicting water “quantity” in sufficiently
200 large and data rich catchments.



201 While this is, from a management perspective, a significant success story, these conceptual
202 models have severe limitations. A serious one is that their successful application does not
203 convincingly explain why a catchment responds the way it does. A statement like: “This is
204 because the beta parameter is 0.9” is not very insightful, as conceptual model parameters
205 cannot, despite numerous regionalization efforts (He et al., 2011a), be related to measurable
206 catchment characteristics in a unique and generalizable manner. Of course, we acknowledge
207 that regionalization functions maybe derived successfully, which, for example, relates the beta
208 of the HBV soil moisture accounting scheme to soil type and land use (as shown by, e.g.,
209 Hudecha and Bardossy, 2004; Samaniego and Bardossy, 2006; He et al., 2011b; Singh et al.,
210 2016), but such relations remain specific to the landscape of interest. Savenije (2010) and
211 Fencia et al. (2011) partially overcame this limitation in their flexible model framework, by
212 subdividing the landscape into different functional units (plateaus, hillslopes, wetlands,
213 rivers), representing each of them by a specific combination of conceptual model components
214 to mimic their dominant runoff generation. Landscapes with different dominant runoff
215 generation mechanisms are represented through an appropriate combination of these
216 conceptual “building blocks” (Fencia et al., 2014; Gao et al., 2014; Wrede et al., 2015), and
217 the fraction of wetlands can be determined using topographical signatures such as “Height
218 Above Next Drainage” (Gharari et al., 2011). While this is a clear advance toward models that
219 predict the effect and also provide a cause, the explanations are still highly abstract, as the
220 visualisation of the conceptual building blocks for plateaus or hillslope looks more like an
221 electrical circuit diagram. From the previous arguments, we conclude that the
222 complexity of hydrological systems does not vanish when expressing hydrological processes
223 in mathematically simple terms. Rather, the complexity is simply shifted to parameter search
224 and regionalization, both of which are highly mathematically demanding.

225 The application of conceptual models becomes inherently questionable when considering
226 catchments smaller than 20 km². These systems are dominated largely by hillslope scale
227 interactions (Robinson and Sivapalan, 1995; Loritz et al., 2017, 2018), including vertical and
228 lateral preferential flow, partly at the bedrock interface, extending across the entire hillslope
229 (Tromp-van Meerveld and McDonnell, 2006a, 2006b; Wienhofer et al., 2009). The small
230 system sizes lead to the result that errors arising from simplified concepts do not simply
231 average out, as they tend to do at much larger scales (Dooge, 1986). Lumped conceptual
232 models are not particularly helpful to predict water quality. This is because they cannot, by
233 definition, account for the above-mentioned physical and structural controls of fluid velocities
234 and travel time distributions of water feeding stream flow.

235 A well-known – and controversial – avenue to close these gaps is to make use of
236 physically-based hydrological models such as MikeShe (Refsgaard and Storm, 1995; Feyen et
237 al., 2000) or CATHY (Camporese et al., 2010). Typically, these models rely on the Darcy–
238 Richards equation, the Penman–Monteith equation for soil-vegetation-atmosphere exchange
239 processes, and the Saint–Venant equations for overland and stream flow. Reactive transport is
240 simulated by the advection-dispersion equation (e.g., Šimunek et al., 1999; Gärdenäs et al.,
241 2006; Gassmann et al., 2013), or particle tracking schemes (Klaus and Zehe, 2011; Roth and
242 Hammel, 1996; Hammel and Roth, 1998). However, the value of physically-based
243 hydrological models has been questioned (Beven, 1989; Savenije and Hrachowitz, 2017) ever
244 since the idea of their existence was proposed by Freeze and Harlan (1969). Moreover,



245 applications of physically-based models are also subject to equifinality (Binley and Beven,
246 2003; Klaus and Zehe, 2010).

247 While each of these approaches is subject to limitations, use of the Darcy-Richards
248 receives by far the strongest criticism (Kirchner, 2006; Beven and Germann, 2013). This is
249 because the key underlying assumption regarding the dominance of capillarity-controlled
250 diffusive flow, under local equilibrium conditions, is largely inappropriate when accounting
251 for preferential flow. Several approaches have been proposed to close this gap, based on (a)
252 stochastic convection assuming no mixing at all (Simmons, 1982), to (b) dual-permeability
253 conceptualizations relying on overlapping, exchanging continua (Šimunek et al., 2003), to (c)
254 spatially explicit representations of macropores as connected flow paths (Vogel et al., 2006;
255 Sander and Gerke, 2009; Zehe et al., 2010; Wienhoefer and Zehe, 2014; Loritz et al., 2017),
256 and to (d) pore-network models based on mathematical morphology (Vogel and Roth, 2001).
257 An alternative to deal with preferential flow and transport are Lagrangian models such as
258 SAMP (Ewen, 1996a,b), MIPs (Davies and Beven, 2012; Davies et al., 2013), and LAST
259 (Zehe and Jackisch, 2016; Jackisch and Zehe, 2018; Sternagel et al., 2019). While each of
260 these concepts has particular strengths and weaknesses (e.g., Šimunek et al., 2003; Beven and
261 Germann, 2013), none of them has been accepted broadly. This explains why attempts to
262 assess travel and residence time distributions from physically-based model simulations
263 (Heidbuchel et al., 2013; Jing et al. 2019) are the subject of controversial discussion.

264 As an alternative, the isotope community focuses on inference of travel time distributions
265 from stable isotopes or tritium concentrations in rainfall and stream flow. Originally, stable
266 isotopologues of the water molecule gained attention as they allow a separation of the storm
267 hydrograph into pre-event and event water fractions (Bonell et al., 1990; Sklash et al., 1996).
268 They are now used commonly as a continuous source of information about travel time
269 distributions of water that enters the catchment via precipitation and is released as streamflow
270 (McGlynn et al., 2002; McGlynn and Seibert, 2003; Weiler et al., 2003; Klaus et al., 2013).
271 Travel time distributions inferred from isotopes are essentially time dependent (Klaus et al.,
272 2015), which raises the question of whether or not this reflects a state-dependent distribution
273 of fluid velocities (Hrachowitz et al., 2013). Travel time models are also used to simulate
274 stream concentration of tracers, either by means of convolution (Rinaldo et al., 2015) or by
275 solving the catchment water balance equation for each age (also called the "Master Equation";
276 see Sect. 3.3) at every time (Botter et al., 2011). By doing so, catchment storage is also
277 calculated from the catchment water balance. This method has been applied in several recent
278 studies (e.g. Harman, 2015; Benettin and Bertuzzo, 2018; Rodriguez et al., 2018). Solving the
279 Master Equation requires an assumption about the shape of the StorAge Selection function
280 (Harman, 2015). The latter is the integral of the travel time distribution over all water ages.
281 Travel time distributions but also StorAge Selection functions are often assumed to be gamma
282 distributed, or a superposition of several gamma distributions (Hrachowitz et al., 2010; Klaus
283 et al., 2015; Rodriguez et al., 2019).

284 In this context, it is interesting to recall that catchments were modelled as time invariant,
285 linear systems in early studies (Sherman, 1932). The runoff coefficient was used to calculate
286 the effective precipitation, while runoff concentration was simulated by convoluting effective
287 precipitation with the system function or greens function, which is the catchment response to
288 a delta input of rainfall. A popular means to assess this well-known "unit hydrograph" is to



289 conceptualize a catchment as a single liner reservoir or a cascade of linear reservoirs. The
290 latter is named after Nash, who showed that the corresponding system function is
291 mathematically equivalent to a gamma distribution (Nash, 1957). The Nash cascade is still
292 used widely in engineering hydrology (Bardossy, 2007). As runoff concentration operates
293 along surface and subsurface preferential pathways, one might hence wonder whether
294 preferential flow implies generally gamma distributed travel times. We address this key
295 question in depth in Sect. 3.4.

296 **2.2 The critical zone: Mediator between two water worlds**

297 The soil-vegetation-atmosphere-transfer system (SVAT-system), or in more recent terms,
298 the “critical” zone, is the mediator between the atmosphere and the two water worlds. This
299 tiny compartment controls the splitting of rainfall into overland flow and infiltration, and the
300 interplay among soil water storage, root water uptake and groundwater recharge. Soil water
301 and soil air contents control CO₂ emissions of forest soils, denitrification and related trace gas
302 emissions into the atmosphere, as well as biogeochemical transformations of chemical
303 species.

304 Partly saturated soils may, depending on initial their state and structure, respond with
305 preferential flow and transport of contaminants and nutrients through the biological most
306 active topsoil buffer (Flury et al., 1994, 1995; Flury, 1996; McGrath et al., 2008, 2010; Klaus
307 et al., 2014). Rapid transport operates within strongly localized preferential pathways such as
308 root channels, cracks, worm burrows or within connected inter-aggregate pore networks
309 which “bypass” of the soil matrix continuum (e.g., Beven and Germann, 1982; Blume et al.,
310 2009; Beven and Germann, 2013). The well-known fingerprint of preferential flow is a
311 “fingered” flow pattern, which is often visualised through dye staining or two-dimensional
312 concentration patterns in vertical soil profiles (Fig. 2). These reveal an imperfectly mixed
313 transport stage in the “near field” at a fixed time, which implies a non-Gaussian, fat-tailed
314 travel distance distribution of solutes.

315 The fact that such preferential flow patterns cannot be reproduced with simulations that
316 combine the Richards equation with the advection-dispersion equation has been discussed for
317 more than 30 years (e.g., Beven and Germann, 1982, 2013). A recent study (Sternagel et al.,
318 2019) revealed that even double domain models such as Hydrus 1D may fail to match the
319 flow fingers and/or long-time concentration tails in tracer profiles. Frequently, the partially
320 saturated region of the subsurface is simply too thin to allow perfectly mixed Gaussian
321 concentrations to be established; these non-Gaussian distributions are today regarded as being
322 the rule rather than the exception.

323



Germany, van Schaik et al. (2014) Chile, Blume et al. (2009) Austria, Wienhöfer et al. (2009)



Germany, Zehe and Flüher (2001) Switzerland, Flury et al. (1994)



324
325
326
327
328
329
330
331
332

Figure 2 Finger flow pattern revealed from standardized dye staining experiments for a transport time of 1 day; images were generously provided by Flury et al. (2004; 2005; Copyright © 1994, 1995 the American Geophysical Union) for Switzerland, Blume et al. (2009, Copyright © Theresa Blume) for Chile, Wienhöfer et al. (2009, Copyright © Jan Wienhöfer KIT) for Austria, and Zehe and Flüher (2001, Copyright © Erwin Zehe KIT) and van Schaik et al. (2014, Copyright © 2013 John Wiley & Sons, Ltd.) for the German Weiherbach.

333 Because preferential transport leads to strongly localized accumulation of water and
334 chemical species, preferential pathways are potential biogeochemical hotspots. This is
335 particularly the case for biopores such as worm burrows and root channels. Worm burrows
336 provide a high amount of organic carbon and worms “catalyse” microbiological activity due
337 to their enzymatic activity (Bundt et al., 2001; Binet et al., 2006; Bolduan and Zehe, 2006;
338 van Schaik et al., 2014). Similarly, plant roots provide litter and exude carbon substrates to
339 facilitate nutrient uptake. Intense runoff and preferential flow events optionally connect these
340 isolated “hot spots” to lateral subsurface flow paths such as a tile drain network or a pipe
341 network along the bedrock interface, and thereby establish “hydrological connectivity”
342 (Tromp-van Meerveld and McDonnell, 2006b; Lehmann et al., 2007; Faulkner, 2008). The
343 onset of hydrological connectivity comprises again a “hot moment” as upslope areas and,
344 potentially, the entire catchment start “feeding” the stream with water, nutrients and
345 contaminants (Wilcke et al., 2001; Goller et al., 2006).

346 The critical zone, furthermore, crucially controls the Bowen ratio (the partitioning of net
347 radiation energy into sensible and latent heat), and soil water available to plants is a key
348 controlling factor. The residual soil water content is not available for plants, as it is stored
349 generally in fine pores subject to very high adhesive forces; this water is rather immobile and
350 likely very “old”. Isotopic tracers have been fundamental to unravelling water flow paths in
351 soils, using dual plots (Benettin et al., 2018; Sprenger et al., 2018), and to distinguish soil



352 water that is recycled to the atmosphere and released as stream flow (Brooks et al., 2010;
353 McDonnell, 2014).

354 Further to the above points, it is noted that laboratory and numerical studies of multiple
355 cycles of infiltration-drainage of water and chemicals into a porous medium demonstrate
356 clearly the establishment of stable “old” water clusters/pockets, and even a “memory effect”
357 (Kapetas et al., 2014), which remain even with multiple cycles of “new” water infiltration
358 (Gouet-Kaplan and Berkowitz, 2011). These pore-scale studies are in qualitative (and semi-
359 quantitative) agreement with studies at the *field scale*, which show similar retention behaviour
360 of bromide (introduced during the first infiltration cycle) after multiple infiltration-drainage
361 cycles (Turton et al., 1995; Collins et al., 2000). As a consequence, when each cycle of
362 infiltration contains water with a different chemical signature, stable pockets of water can be
363 established with highly varying chemical composition.

364 In this context, then, we emphasise that mobile and immobile waters – and the chemical
365 species they contain – exist at a continuum of scales from the pore to the field level. Thus,
366 rather than attempting to delineate pockets of less and more mobile water at each scale –
367 separating these pockets at the pore, the column, the meter, the 10 meter, and the field and
368 catchment scales – we instead suggest recognising and delineating an “overall effect” of
369 separation between “old” (immobile) and “new” (mobile) waters at a given “effective” scale
370 of interest, which integrates over all such old and new waters. Moreover, we emphasise that
371 highly mobile and less mobile regions for soil water can be in close proximity and yet still be
372 located in distinctly different pore size fractions, which implies highly different fluid
373 velocities and thus water ages. Surface vegetation may easily tap these water pockets, but it
374 will also tap the young ages in larger pores because less physical work is required during root
375 water uptake (Hildebrandt et al., 2016). Thus, the idea of a distinct separation of waters (e.g.,
376 Brooks et al., 2010) – one type supplying runoff and the other supplying transpiration – is a
377 highly idealized interpretation of soil physics and the inherently low degrees of freedom
378 associated with water mixing across pore size fractions (Zehe and Jackisch, 2016).

379 Simply put, we have two different forms of water release – stream flow generation and
380 transpiration – and contributions of water and chemical species with a range of signatures. But
381 just as we cannot separate pore-scale old-new (immobile/mobile) water contributions at the
382 large scale, we have a similar difficulty at all scales. As we discuss in detail in Sect. 3, then,
383 we argue that it is a more effective approach to consider chemical transport as following
384 *distributions of travel distances and residence times*, which can then characterized by various
385 (often power law) probability density functions.

386 2.3 Groundwater systems

387 As noted in Sect. 1, analysis of groundwater systems has developed largely independently
388 of investigation of surface water systems, although it, too, developed originally as a large
389 deterministic engineering discipline around the traditional task of water supply for domestic
390 and agricultural use. It was only in the 1980’s that “stochastic” (probabilistic and statistical)
391 techniques began to be implemented extensively, to account for the many uncertainties
392 associated with aquifer structure and hydraulic properties that control the flow of
393 groundwater. In parallel, significant interest (and concern) with water quality and
394 environmental contamination in groundwater systems only entered the research community’s



395 consciousness in the 1980s, although some pioneering laboratory experiments and field
396 measurements were initiated from the late 1950s.

397 It is worth noting, too, that the methods and models applied in groundwater research
398 developed independently and separately from research on surface water systems (Sect. 1). The
399 only partial connection or “integrator” has traditionally been with aquifer connections to the
400 vadose zone (or critical zone, discussed in Sect. 2.2). Another connection between surface
401 water and groundwater systems, though not generally recognized as such, has been analysis of
402 water flow, and to a lesser extent chemical species transport, in the hyporheic zone. The
403 hyporheic zone can be defined as the region of sediment and subsurface porous domain below
404 and adjacent to a streambed, which enables mixing of shallow groundwater and surface water.
405 (e.g., Haggerty et al, 2002).

406 To quantify chemical transport, landmark laboratory experiments (e.g., Aronofsky and
407 Heller, 1957; Scheidegger, 1959) measured breakthrough of conservative (non-reactive)
408 chemical tracers through columns of sand. These measurements underpinned theoretical
409 developments, based also on concepts of Fickian diffusion, which led to consideration of the
410 classical advection-dispersion equation. Since that time, the advection-dispersion equation –
411 and variants of it – have been used extensively to quantify chemical transport in porous
412 media. However, as thoroughly discussed in Berkowitz et al. (2006), solutions of the
413 advection-dispersion equation have repeatedly demonstrated an inability to properly match
414 results of extensive series of laboratory experiments, field measurements, and numerical
415 simulations. These findings naturally lead to the conclusion that the conceptual picture
416 underlying the advection-dispersion equation framework is insufficient. Stochastic variants of
417 the advection-dispersion equation, and implementation of multiple-continua, advection-
418 dispersion equation formulations (including mobile-immobile models) have been used to
419 provide insights into factors that affect chemical transport – particularly given uncertain
420 knowledge of detailed structural and hydraulic aquifer properties – but they have been largely
421 unable to capture measured behaviours of chemical transport. This observation is largely in
422 line with what we reported for the critical zone.

423 The first key is to recognize that heterogeneities are present at all scales in groundwater
424 systems, from sub-millimetre pore scales to the scale of an entire aquifer. Indeed, use of the
425 term “heterogeneities” refers to varying distributions of structural properties (e.g., porosity,
426 presence of fractures and other lithological features), hydraulic properties (e.g., hydraulic
427 conductivity), and in the case of chemical transport, variations in the biogeochemical
428 properties of the porous domain medium. The second key is to recognize that these variations
429 in distributions, at all scales, deny the possibility of obtaining complete knowledge of the
430 aquifer domain in which fluids and chemical species are transported. A third key, when
431 considering chemical transport, is to recognize that chemical species are subject to several
432 critical transport mechanisms and controls, in addition to advection, that do not affect flow of
433 water – molecular diffusion, dispersion, and reaction (sorption, complexation, transformation)
434 – so that chemical migration through an aquifer is influenced strongly by aquifer
435 heterogeneities and initial/boundary conditions. Extensive analysis of high-resolution
436 experimental measurements and numerical simulations of transport demonstrate that small-
437 scale heterogeneities can significantly affect large-scale behaviour, and that small-scale

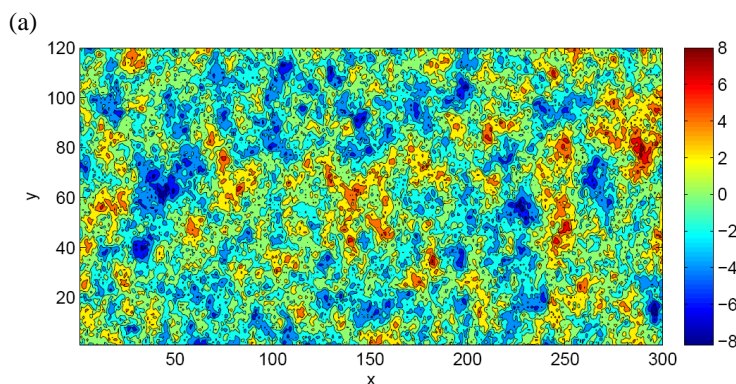


438 fluctuations in chemical concentrations do not simply average out and become insignificant at
439 large scales.

440 As discussed in the preceding sections, preferential pathways are ubiquitous and affect
441 both water and chemical species, resulting from system heterogeneity. To be more specific,
442 (local) hydraulic conductivities vary in space over orders of magnitudes, even within
443 distances of centimetres to meters, and these variations ultimately control patterns of fluid and
444 chemical movement. The resulting patterns of movement in these systems involve highly
445 ramified preferential pathways for water movement and chemical migration. To illustrate
446 these points, consider the hydraulic conductivity (K) and preferential pathway maps shown in
447 Fig. 3a; see Edery et al. (2014) for full details.

448 Figure 3a shows a numerically-generated, two-dimensional domain measuring 300×120
449 discretized into grid cells of uniform size (0.2 units). The K -field shown here was generated as
450 a random realization of a statistically homogeneous, isotropic, Gaussian $\ln(K)$ field, with
451 $\ln(K)$ variance of $\sigma^2 = 5$. Fluid flow through this domain was solved at the Darcy level by
452 assuming constant head boundary conditions on the left and right boundaries, and no-flow
453 horizontal boundaries; the hydraulic head values determined throughout the domain were then
454 converted to local velocities, and thus streamlines. Chemical transport was determined using a
455 standard Lagrangian particle tracking method, with 10^5 particles representing the dissolved
456 chemical species. Particles advanced by advection along the streamlines and molecular
457 diffusion (enabling movement between streamlines), to generate breakthrough curves
458 (concentration vs. time) at various distances along the domain. Figure 3b shows particle
459 pathways through the domain, wherein the number of particles visiting each cell is
460 represented by colours. The emergence of distinct, limited particle preferential pathways from
461 inlet boundary to outlet boundary is striking. Notably, too, there are significant regions that
462 remain free of particles (the white regions in Fig. 3b), and preferential pathways are confined
463 and converge between low conductivity areas. Even more striking is set of even sparser
464 preferential pathways shown in Fig. 3c: here, only cells, which were visited by at least 0.1%
465 of all injected particles, are shown. In other words, 99.9% of all chemical species migrating
466 through the domain shown in Fig. 3a advance through a limited number and spatial extent of
467 preferential pathways. It is significant, too, that the preferential pathways comprise a
468 combination of higher conductivity cells the paths, but also some low conductivity cells, as
469 reported also in Bianchi et al. (2011); see Sect. 3.1 for further discussion of this behaviour.

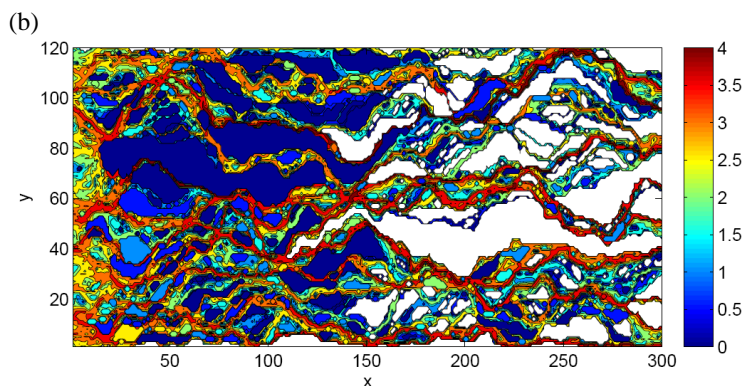
470
471



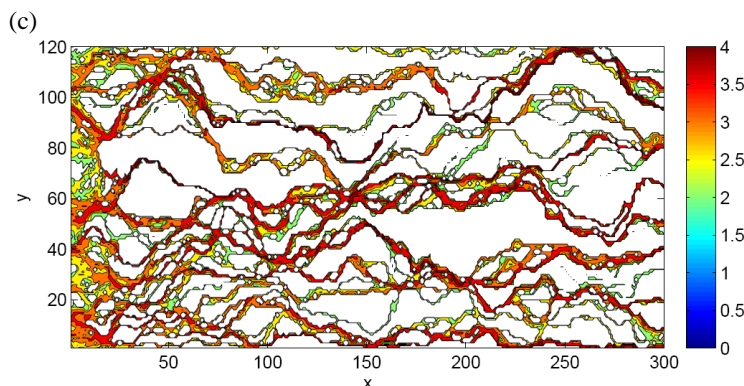
472



473



474
475



476
477

Figure 3 (a) Spatial map showing a sample hydraulic conductivity (K) field generated statistically (right side bar shows scale of $\ln(K)$). (b) Spatial map showing particle paths through the domain, for overall hydraulic gradient (water flow) from left to right. “Particles” representing dissolving chemical species are injected along the left vertical boundary and followed through the domain. White regions indicate where *no* particles “visit” (interrogate) the domain. Blue regions have only a small number of particle visitations. Red regions have significant particle visitations. Note that the colour bar is in \log_{10} number of particles. (c) Spatial map showing particle paths *preferential* particle paths, defined as paths through cells (underlying subdivisions in the domain, each with a different K value as shown in plot (a) above) that each contain a “visitation” of a minimum of 0.1% of the total number of particles in the domain. Note that the colour bar is in \log_{10} number of particles (after Ederly et al., 2014; Copyright 2014, with permission from the American Geophysical Union).

490

Thus, it is clear that the groundwater systems incorporate regions of water – distributed throughout the domain – that may have very different chemical signatures, even in close proximity to each other. Moreover, these regions can be relatively stable over time, modified only by the extent of chemical diffusion into and out of the “immobile” regions.

495

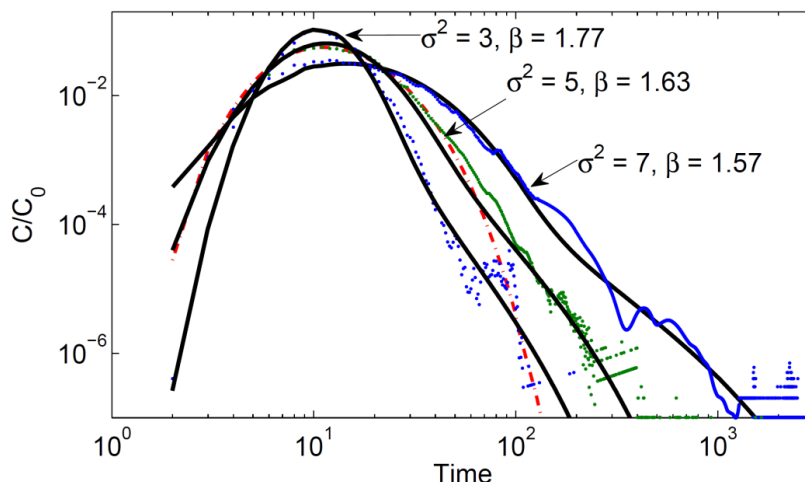
Considering now arrival times of chemical species at the domain outlet boundary, Fig. 4 shows the relative concentration (C/C_0) vs. time – breakthrough curves – for three degrees of domain heterogeneity ($\ln(K)$ variance). It is evident that the chemical transport in this domain displays “non-Fickian” (or “anomalous”) transport, in the sense that late-time (long tail) arrivals are registered at the measurement plane. Furthermore, Fickian-based advection-

499



500 dispersion equation models clearly fail to quantify such behaviour. However, Fig. 4 shows
501 solutions – based on the continuous time random walk (CTRW) framework – that do
502 effectively describe the chemical transport. The CTRW framework and governing transport
503 equations are detailed in Sect. 3.3).

504
505



506
507 **Figure 4** Breakthrough curves (points) for three $\ln(K)$ variances ($\sigma^2 = 3, 5, 7$; 100 realizations
508 each), (a) at the domain outlet ($x = 300$ length units), and corresponding CTRW fits (curves).
509 Also shown is a fit of the advection-dispersion equation (dashed-dotted curve), for $\sigma^2 = 5$.
510 See Sect. 3.3 for further discussion and explanation of β . All values are in consistent, arbitrary
511 length and time units (after Ederly et al., 2014; Copyright 2014, with permission from the
512 American Geophysical Union).

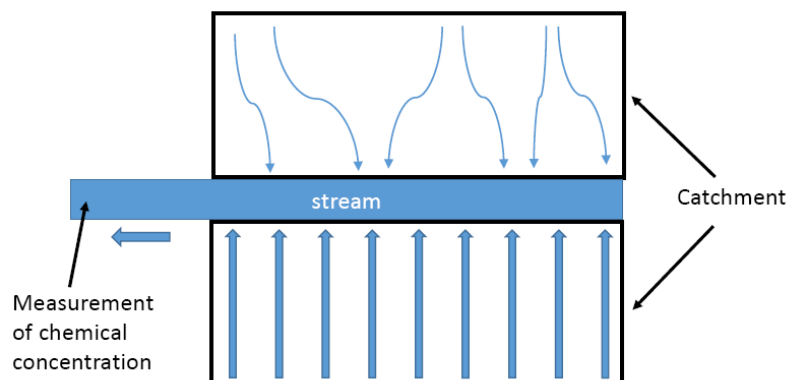
513 3 MERGING TREATMENT OF SURFACE WATER AND 514 GROUNDWATER SYSTEM TRANSPORT DYNAMICS

515 3.1 Conceptual pictures, travel times, and mixtures of water with different chemical 516 signatures

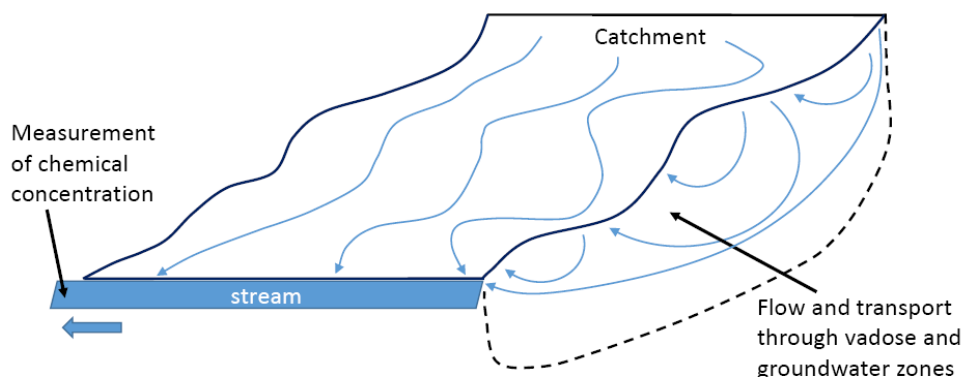
517 Clearly, any quantitative model of fluid flow and chemical transport in a catchment must
518 first define a conceptual picture. In the context of the discussion in Sects. 2 and 3 that led us
519 to this point, we require a picture that accounts naturally for overland and interacting
520 subsurface flow and transport, recognizing the ubiquity of preferential pathways and a broad
521 (and often different) distributions of fluid and chemical travel times. Moreover, any such
522 conceptual picture also requires definition of the available measurement benchmark against
523 which a quantitative model can be compared. In the case of catchments, a common
524 measurement is that of chemical arrival times at a downstream sampling point in a catchment
525 stream that drains and exits the catchment. Thus, the dynamics of fluid flow and chemical
526 transport in a fully three-dimensional (or simplified two-dimensional overland) catchment are
527 often represented by measurements in an effective, spatially averaged one-dimensional



528 system. (Of course, higher resolution, multidimensional (in space) measurements, if available,
529 should also be considered in a quantitative model!)
530



531
532 (a)
533



534
535 (b)
536

537 **Figure 5** Conceptual pictures of water flow and chemical transport in catchments under a pulse of rainfall over the entire catchment. Each curved arrow (or idealized straight arrow)
538 indicates a different path, each of which embodies different travel times through the system
539 until reaching the stream. Note that each preferential pathway carrying water and chemical
540 species may be purely overland, or include interactions and advance within soil layers
541 (partially saturated, or vadose, zone) and saturated groundwater systems. (a) Schematic
542 showing idealized 2D catchment area. Arrows through two rectangular regions of catchment
543 indicate a range of preferential pathways carrying water and chemical species. (b) Schematic
544 showing idealized 3D catchment area, under a pulse of rainfall over the entire catchment.
545
546

547 Figures 5a and 5b show, schematically, 2D and 3D conceptualizations of preferential
548 pathways, with associated varying travel times, for both fluid flow and chemical transport.
549 We stress here – and as discussed below in Sect. 3.3 – that the larger scale, effective (or
550 “characteristic”, or average) fluid velocities and chemical species transport velocities need not



551 be identical. In fact, these two velocities are rarely the same, as a consequence of the ubiquity
552 of preferential pathways for water and migrating chemical species in any surface water and/or
553 soil-aquifer domain. Because of these pathways, regions of higher and lower hydraulic
554 conductivity (fluid and chemical mobility) – and thus the entire system – interrogated by
555 water and chemical species differ. While both water molecules and chemical species are
556 subject to diffusive and dispersive transport mechanisms, in addition to advection, chemical
557 species are clearly identifiable while water molecules are not tagged; thus the effects of
558 diffusion and dispersion on “bulk water” transport are invisible and irrelevant. In this context,
559 too, while the surface water literature uses the term “celerity” to describe the speed at which a
560 wave/signal (or “disturbance”) is transmitted through the medium, we point out that but
561 celerity is distinct from chemical transport velocity. A pressure wave, for example, can create
562 a gradient at an aquifer-stream interface that may result in the release of water and chemicals
563 that are close to this interface; however, for the reasons noted above, this does not mean that
564 (average) fluid and chemical transport velocities are identical.

565 The conceptual picture discussed here is our basis for arguing that we should expect to
566 find distributions of travel times and mixtures of water with different chemical signatures, *at*
567 *all scales*. Moreover, these considerations align with some surface water literature, such as
568 cited at the end of Sect. 2.1, which clearly recognizes the occurrence of wide distributions of
569 water and chemical travel times, and long-term chemical persistence in water catchment
570 storage (e.g., Niemi, 1977; Botter et al., 2010, 2011; Hrachowitz et al., 2010; McDonnell and
571 Beven, 2014; Kirchner, 2016).

572 As pointed out in Sect. 2, several studies in recent years have specifically reported the
573 presence of water bodies (or pockets, or regions, depending on scale), with different chemical
574 compositions and isotopic signatures, that are in close proximity or even “overlapping” (in
575 some sense). Some authors use the term “two water worlds” – immobile and mobile – in this
576 context (e.g., Brooks et al., 2010; Evaristo et al., 2015). In light of the discussion in Sect. 2,
577 we stress here that the conceptual picture to explain spatially and temporally varying chemical
578 compositions (in subsurface, soil, sediment and aquifer systems), and associated uptake by
579 vegetation, is subtle. We question the conceptualization of two (or more) *separate, fully*
580 *compartmentalized* mobile and immobile regions of water and chemicals. We argue that
581 mobile and immobile regions are more appropriately considered as overlapping continua or
582 ensemble/effective averages, as those are found at all scales from pores to hundreds of meters
583 (e.g., Turton et al., 1995; Collins et al., 2000; Gouet-Kaplan and Berkowitz, 2011; recall Sect.
584 2.2). We therefore expect to find mixtures of travel times and waters with different chemical
585 signatures, *at all scales*, and argue that it is preferable to think in terms of time, so there is a
586 range of overlapping temporal (transition time) distributions that each contribute to the
587 overall, large-scale fluid flow and chemical transport. This leads naturally to the CTRW
588 framework.

589 **3.2 Space vs. time: the travel time perspective of transport**

590 It is critical to point out that in all of the figures shown above in Sects. 2.1 and 2.3, the
591 *residence times* of water and chemicals are the key factors that determine transport behaviour.
592 This leads to the continuous time random walk (CTRW) framework, which operates more (or
593 at least equally!) in terms of time than in terms of space (see Sect. 3.2). To introduce CTRWs,



594 in the context of the pathway “self-organisation” shown in Fig. 4c, we demonstrate the
595 importance of thinking in terms of *time* rather than *space*. Consider the simple example of
596 driving a distance of 100 km; we consider a scenario in which we travel 50 km at 1 km/h, and
597 then 50 km at 99 km/h. The average speed of travel, in terms of *space* (distance), is
598 determined as follows: given that we travelled 50 km at each of two speeds, the average speed
599 is $(1 + 99) / 2 = 50$ km/h. Thus, with this calculation, the total time to travel 100 km “should”
600 be 2 h. However, the *actual* time taken to travel this distance – 50 km at 1 km/h, and then 50
601 km at 99 km/h – is 50.5 h. In other words, traditional (but incorrect!) conceptual spatial
602 thinking highlights the erroneous effects of focusing only on *spatial* heterogeneity and
603 quantification based only on spatial characteristics.

604 In a similar analogy, it is sometimes faster to pass through a bottleneck region (e.g., drive
605 for a short time through a very narrow and slow road) to ultimately reach a fast highway,
606 rather than to travel at medium speed along a road for an entire journey.

607 Another aspect related to misplaced emphasis on spatial heterogeneities, is also noted
608 here. Referring again to the preferential pathways show in Fig. 3c, it is seen that these
609 pathways actually contain some low hydraulic conductivity (K) regions as well! This can be
610 explained most easily, conceptually, in terms of one-dimensional pathways. Consider a
611 number of high and low K cells in series, [3 3 3 3 3] vs. [6 6 1 6 6], where the
612 effective/average K is given by the harmonic mean. While a [3 3 3 3 3] series may appear to
613 enable a greater volumetric flow rate than a [6 6 1 6 6] series, due to the “bottleneck” low K
614 value in the center, both series in fact have the same harmonic mean ($=3$) and conduct fluid
615 equally well.

616 A similar argument can be applied to analysis of land topography and surface water flow.
617 The “high resistance” (in principle, but not necessarily), localized small ‘humps of roughness
618 elements’, and surface tension effects – analogous to the low K cells given in the previous
619 paragraph – can be overcome, to allow development of preferential pathways that do not
620 always follow the path of steepest descent in terms of surface topography. There are thus
621 small bypassing effects. Moreover, there is flow/transport from land surface into the
622 subsurface (e.g., hyporheic zone), which also “bypasses” localized small “humps” in the land
623 surface and allows fluid connection/communication further downstream (along a pathway).
624 As a consequence, we argue that it is misleading to place undue focus on the high resistance
625 (or surface “hump”) bottlenecks; rather, it should be recognized that entire “high K ” or
626 “potential” regions for flow are often unsampled or barely sampled by flowing water and
627 chemicals, at least over moderate time scales.

628 In the next section, we adopt a temporal framework to introduce continuous time random
629 (CTRW) theory, which is the basis of our proposed means to unify quantification of
630 groundwater and surface water transport dynamics.

631 3.3 Continuous Time Random Walks: Theory

632 Preferential flow leads to non-Fickian (or “anomalous”) travel time distributions and rapid
633 breakthrough (and/or long tailing) of chemical species in heterogeneous domains. The travel
634 time (residence time) perspective of transport, and consideration of hydrological systems as
635 imperfectly mixed reactors, are incorporated naturally with the continuous time random walk
636 (CTRW) framework.



637 Detailed descriptions of CTRW can be found in, e.g., Berkowitz et al. (2006, 2016). Here,
638 we present only a brief outline of the essential elements. The CTRW framework is based on
639 direct incorporation of the distribution of flow field fluctuations and thus of the fluctuations in
640 concentrations of transported chemicals. As such, the CTRW is a time-nonlocal approach that
641 can quantify chemical transport over a range of length (and time) scales, and address other
642 processes such as chemical reactions.

643 “Particles”, representing dissolved chemical species, are used to treat chemical transport;
644 particles undergo spatiotemporal transitions that encompass both displacement due to
645 structural heterogeneity and the time taken to make the particle movement. Unlike other
646 approaches, the formulation focuses on retaining the full distribution of transition times. Thus,
647 CTRW defines a probability density function (PDF), $\psi(\mathbf{s}, t)$, of a random walk that couples
648 the spatial displacement \mathbf{s} and time t of the transition. As shown in Dentz et al. (2008), it is
649 convenient and generally applicable (but not obligatory) to use the approximation $\psi(\mathbf{s}, t) =$
650 $p(\mathbf{s})\psi(t)$, where $\psi(t)$ is the probability rate for a transition time t between sites, and $p(\mathbf{s})$ is the
651 probability distribution of the length of the transitions.

652 The defining transport equation is equivalent to a generalized master equation (GME),
653 which is essentially a mass balance equation in space and time. Using a Taylor expansion, the
654 GME can be transformed into the continuum version (ensemble-averaged system) of the
655 CTRW, in the form of an integro-partial differential equation:

$$656 \frac{\partial c(\mathbf{s}, t)}{\partial t} = \int_0^t dt' M(t - t') [-\mathbf{v}_\psi \cdot \nabla \tilde{c}(\mathbf{s}, t') + \mathbf{D}_\psi : \nabla \nabla \tilde{c}(\mathbf{s}, t')] \quad (1)$$

658
659 for the normalized concentration $c(\mathbf{s}, t)$, where M is a memory function, the transport velocity
660 \mathbf{v}_ψ and the generalized dispersion \mathbf{D}_ψ are defined in terms of the first and second moments of
661 $p(\mathbf{s})$, and with the dyadic symbol $:$ denoting a tensor product. In Laplace space, (1) becomes

$$662 \quad 663 \quad u\tilde{c}(\mathbf{s}, u) - c_o(\mathbf{s}) = -\tilde{M}(u)[\mathbf{v}_\psi \cdot \nabla \tilde{c}(\mathbf{s}, u) - \mathbf{D}_\psi : \nabla \tilde{c}(\mathbf{s}, u)] \quad (2)$$

664
665 where the memory function $\tilde{M}(u) \equiv \bar{t}u\tilde{\psi}(u)/[1 - \tilde{\psi}(u)]$, \bar{t} is a characteristic time, and with
666 \sim denoting Laplace space and u denoting the Laplace variable. Note that this continuum
667 formulation contains a nonlocal-in-time convolution, in terms of the memory function.

668 In contrast to the classical advection-dispersion equation (see Eq. (4), below), the
669 “transport velocity,” \mathbf{v}_ψ is in principle distinct from the “average fluid velocity,” \mathbf{v} . This is
670 because chemical transport is subject to diffusive and dispersive mechanisms, so that the
671 effective, overall transport (i.e., a “characteristic” velocity) of chemical may be faster or
672 slower than the average fluid velocity. (Recall, too, the discussion in Sect. 3.1 regarding the
673 distinction between celerity and chemical transport.) We point out, moreover, that residence
674 times are a key characterisation, as they generally differ for water and chemical species. To
675 illustrate, it is sufficient to recognise that the preferential flow paths themselves are generally
676 stable when the overall hydraulic gradient changes (unless dealing with significant changes or
677 turbulent flow), so that the residence time dictates the relative influence of diffusion and
678 chemical movement into and out of less mobile zones, which ultimately affects breakthrough
679 curves (Berkowitz and Scher, 2009).



680 It is critical to recognize that the occurrence of “rare events” – even a small proportion of
681 chemical species migrating extremely slowly in some regions, and/or being repeatedly
682 trapped and released of slow regions over a series of spatial transitions – are sufficient to lead
683 to anomalous transport and extremely long “average” chemical transport times (Berkowitz et
684 al., 2016). Thus, it is important to differentiate between “average” (recall Sect. 3.1) and
685 “effective” transport of “most” particles. Indeed, we emphasise, too, that the effects of these
686 “rare events” are deeply significant: they do not simply average out, but rather propagate to
687 larger time and space scales.

688 The transition time distribution, $\psi(t)$, is thus at heart of the CTRW framework, and its
689 form determines the memory function. As discussed in detail (e.g., Berkowitz et al., 2006,
690 2016), it is expedient to define (t) as a truncated power law (TPL), which enables an evolution
691 to Fickian behaviour:

$$692 \quad \psi(t) = \frac{n}{t_1} \exp(-t/t_2) / (1 + t/t_1)^{1+\beta} \quad (3)$$

693 for $0 < \beta < 2$, with the normalization constant

$$694 \quad n \equiv (t_1/t_2)^{-\beta} \exp(-t_1/t_2) / \Gamma(-\beta, t_1/t_2) \quad (4)$$

695 and with $\Gamma(-\beta, t_1/t_2)$ denoting the incomplete Gamma function (Abramowitz and Stegun,
696 1970). This functional form of $\psi(t)$ has been particularly successful in interpreting a wide
697 range of laboratory and field observations, as well as numerical simulations. We chose the
698 characteristic time appearing in the memory function to be t_1 , which represents the onset of
699 the power law region. The truncated power law form of $\psi(t)$ behaves as a power law
700 proportional to $(t/t_1)^{-1-\beta}$ for transition times in the range $t_1 < t < t_2$; $\psi(t)$ decreases
701 exponentially for transition times $t > t_2$. Thus, the TPL enables quantification of non-Fickian
702 transport, with a finite (sufficiently small) t_2 , it facilitates (where appropriate) a longer-time,
703 smooth evolution to Fickian transport. We note, too, that the CTRW framework also
704 simplifies (e.g., Berkowitz et al., 2006, 2016) to specialized subsets of non-Fickian transport
705 behaviour embodied within, e.g., multirate mass transfer (Haggerty and Gorelick, 1995) and
706 fractional derivative (Zhang et al., 2009) formulations.

707 It is important to recognize, too, that specification of a pure exponential form for $\psi(t)$,
708 namely $\psi(t) = \lambda \exp(-\lambda t)$, with mean $1/\lambda$, and/or choice of $\beta > 2$, reduces the CTRW transport
709 Eq. (1) to the classical advection-dispersion equation, given in a general form as

$$710 \quad \frac{\partial c(\mathbf{s}, t)}{\partial t} = -\mathbf{v}(\mathbf{s}) \cdot \nabla c(\mathbf{s}, t) + \nabla \cdot [\mathbf{D}(\mathbf{s}) \nabla c(\mathbf{s}, t)] \quad (5)$$

711 where $\mathbf{v}(\mathbf{s})$ is the velocity field and $\mathbf{D}(\mathbf{s})$ is the dispersion tensor.

712 It is thus clear that the power law exponent β in $\psi(t)$ characterises the local disorder of the
713 system and the degree of non-Fickian transport as an integral, temporal fingerprint in the
714 breakthrough curves. This reflects the effect of a strongly localised preferential movement of
715 chemical species on travel times (recall Fig. 3), caused by the pattern of local driving



722 gradients and hydraulic conductivity. Because the particle movement is clearly organised in
723 *space*, we suggest that this might be seen as self-organisation: local disorder is manifested in
724 deviation from advective-dispersive transport, which leads to *non-local*, organised dynamic
725 behaviour in *time* at the system scale. This implies that the CTRW framework provides a
726 means to quantify the integral, temporal fingerprint of spatially organised preferential flow
727 through the power law exponent β and the related distance from a Gaussian travel time
728 distribution, as detailed further in Sect. 4.

729 The CTRW transport equation, in partial differential equation form, can be solved in
730 Laplace space (Cortis and Berkowitz, 2005) as well as in real space (Ben-Zvi et al., 2019).
731 One can also solve the transport equation by implementing various particle-tracking
732 formulations. This was done, for example, to obtain the fits to the long-tailed breakthrough
733 curve displayed in Fig. 5. Particle tracking (PT) approaches offer an efficient numerical tool
734 to treat a variety of chemical transport scenarios (for both conservative and reactive chemical
735 species). They are particularly well-suited to accounting for pore-scale to column-scale
736 dynamics. “Particles” (representing chemical mass) advance by sampling transitions in space
737 and time from the associated CTRW distributions. We emphasize that this PT approach can
738 be employed to treat both advection-dispersion equation (Fickian, normal transport) and
739 CTRW (non-Fickian, anomalous transport) formulations, via appropriate choice of
740 (exponential or power law, respectively) $\psi(t)$.

741 The efficacy and relevance of the CTRW framework has been demonstrated extensively
742 for subsurface chemical transport (Berkowitz et al., 2006, 2016; Berkowitz and Scher, 2009;
743 and references therein), from pore to aquifer scales, on the basis of extensive numerical
744 simulations, laboratory experiments and field measurements. The formulation for chemical
745 transport is general and robust over length scales ranging from pore to field, for different flow
746 rates within the same domain, for chemically-reactive species, and even for time-dependent
747 velocity fields (Nissan et al., 2017).

748 To conclude this section, and bridge to discussion that follows in the next section, we
749 point out here that, the *curved power law* form can in some cases be a useful representation
750 rather than the truncated power law (TPL), Eq. (3), as shown by Nissan and Berkowitz
751 (2019). In this case, we write $\psi(t)$ as a curved power law function (Chabrier, 2003)

$$752 \psi(t) = C_1 t^{-1-\beta} \exp(-t^*/t) \quad (6)$$

753 where $C_1 \equiv (t^*)^\beta / \Gamma(\beta)$, is the normalization constant of the probability density function and Γ
754 is the Gamma function. Here, t^* (a characteristic time) controls the exponential increase, while
755 β accounts for the power law region. It is important to note that this curved power law is an
756 *inverse gamma distribution*, with shape parameter β and scale (or rate) parameter t^* . Note that
757 unlike the TPL in Eq. (3), notwithstanding the exponential term in Eq. (6), there is no cut-off
758 time that enables a transition to Fickian transport. These perspectives will be discussed in
759 detail in Sect. 3.3.

762 3.4 Continuous Time Random Walks: Application to Surface Water Systems

763 In the context of our discussion in Sects. 2 and 3.1, recognizing that dynamics of chemical
764 transport in surface water and groundwater systems are at least phenomenologically and



765 functionally/dynamically similar over enormous spatial and temporal scales, we argue there
766 that simulations and analysis using the CTRW framework are meaningful and applicable also
767 to quantifying the (anomalous) dynamics of chemical transport in surface water systems. In
768 both surface water and groundwater systems, there is always “unresolved heterogeneity” (e.g.,
769 hydraulic conductivity, structure) at all scales. Fluid and chemical inputs range from being
770 reasonably well-defined to unknown (e.g., in terms of location and extent of a subsurface
771 contamination leak, areal extent and space-time heterogeneities of rainfall and related stable
772 isotope concentrations), while outputs may also be reasonably well-defined to unknown (e.g.,
773 arrival times of a chemical species to a monitoring point downstream, such as a stream gauge,
774 near surface spring or tile drain outlet). As a consequence, efforts to delineate preferential
775 flow paths and quantify chemical transport must be “adjusted” (or “be appropriate”) to the
776 level of knowledge and spatial/temporal resolution.

777 More specifically, we note that the preferential pathways shown in Fig. 3b,c are
778 (phenomenologically at least) similar to those of surface water systems shown in Fig. 1, while
779 the (temporal) breakthrough curves in Fig. 4 are similar to those determined at stream gauges
780 and tile drain outlets. Clearly, in surface water systems, and throughout small, intermediate
781 and large scales, there are stable regions of “water pockets” (less mobile water) that can be
782 distinguished by strongly varying chemical (ionic, isotopic) compositions. The presence of
783 tributaries leading to rivers in catchments demonstrates clear channelling effects and the
784 establishment of preferential pathways (Sect. 2.1).

785 Moreover, CTRW has also applied in some partially saturated soil-water systems (Sect.
786 2.2), which further strengthens the connection of CTRW to surface water systems; as
787 discussed in Sects. 2 and 3.1 (Figs. 3a,b), surface water flow and associated chemical
788 transport are not purely overland processes, but involve coupled interactions with the partially
789 saturated (vadose) zone (Sect. 2.2) and groundwater zone (Sect. 2.3).

790 Indeed, CTRW methods (and subsets) have already been applied in some sense, at least
791 qualitatively, to interpret anomalous transport in various surface water system scenarios. For
792 example, Boano et al. (2007) used CTRW to quantify chemical transport in a stream,
793 accounting for fluid-chemical interactions with the underlying sediment (i.e., the hyporheic
794 zone). Other studies have recorded power law and related multirate rate mass transfer
795 dynamics for chemical transport in stream and catchment systems (e.g., Haggerty et al., 2002;
796 Gooseff et al., 2003). These authors note, in particular, that the hyporheic zone exhibits an
797 enormous range of time scales over which chemical exchange can occur, with significant
798 amounts of chemical species being retained over extremely long times.

799 However, while full application of CTRW to catchment-scale surface water systems has
800 not been reported to date, there are additional strong indications that it is applicable. We point
801 out two key aspects to support this claim, from the surface water literature. First, as discussed
802 in Sect. 2.1, studies on stable isotope and tritium transport through catchments often rely on
803 the gamma distribution to describe residence times or the StorAge Selection function in
804 catchments. The gamma distribution, used particularly in connection with arrival times of
805 stable isotopes at a catchment outlet (= river outlet, measurement control plane), has been
806 applied to describe the superposition of different functions to account for time dependence
807 (e.g., Hrachowitz et al., 2010). Related directly to this point, too, are unit hydrograph analyses
808 that were used in the past to describe runoff concentration and flood routing, through a Nash



809 Cascade, which is essentially a gamma distribution, as discussed also in Sect. 2.1. We now
810 focus on this aspect in detail.

811 The gamma distribution is given by

812

$$813 \quad P(t) = C_2 t^{-1+\beta} \exp(-t/t^*), \quad (7)$$

814

815 where $C_2 \equiv (t^*)^\beta / \Gamma(\beta)$, or, equivalently (and for comparison to Eq. (6)),

816

$$817 \quad P(t) = C_3 t^{-1+\beta} \exp(-t/t^*), \quad (8)$$

818

819 where $C_3 \equiv 1/[(t^*)^\beta \Gamma(\beta)]$. The gamma distribution describes processes for which the waiting
820 times between Poisson distributed events are important.

821 In light of Sect. 2.1, the choice of a single or a sum of gamma functions (which is also a
822 gamma function) to characterise travel time distributions thus implies a conceptualization of
823 the system, in one or several parallel cascades, of linear reservoirs to representing different
824 flow paths. This in turn rests on the assumption of locally well-mixed conditions within each
825 reservoir, which is questionable in the case of preferential flow, and neglects exchange among
826 these cascades along the flow path. We argue that this is conceptualisation is too idealised,
827 because it does not characterise the full evolution of ubiquitous power law behaviours
828 (transit/arrival times) over long spatial and temporal scales. We suggest that the use of an
829 inverse gamma function (or truncated power law) might improve simulations achieved within
830 past attempts using the gamma function, reported by, e.g., Harman et al. (2015) and
831 Rodriguez et al. (2019, submitted). The former study used a single constant gamma
832 distribution for the StorAge Selection (SAS) function of stream flow and a uniform
833 distribution for evapotranspiration. The corresponding simulation of chloride concentrations
834 in the lower Hafren catchment yielded a Nash Sutcliffe Efficiency (NSE) of 0.54 during
835 calibration, while a storage-dependent SAS improved the calibration to an NSE of 0.66.
836 Rodriguez et al. (2019) used a combination of three gamma functions for the
837 StorAgeSelection function of the Weiherbach catchment, located in Devonian slates in
838 Luxembourg, and the corresponding simulations of stable isotopes concentrations in stream
839 water yielded an NSE of 0.24. The even poorer performance of the three gamma functions in
840 the Weiherbach, located in the Luxembourg Ardennes, likely reflects the higher complexity of
841 the runoff generation process in this landscape (Wrede et al. 2015; Angermann et al., 2017).

842 In the context of considering summations of parallel cascades or travel time distributions,
843 we point out, too, that a power law distribution such as given in Eq. (3) can be approximated
844 by a sum of a sufficient number of exponential distributions, each with a different mean
845 (Berkowitz et al., 2006). In other words, the sum of a series of (exponential) travel time
846 distributions gives an (approximate) power law distribution. Thus, it is appropriate to think in
847 terms of “multiple distributions experienced by different particles”, but with the recognition
848 that the overall contribution of these distributions is in fact a power law.

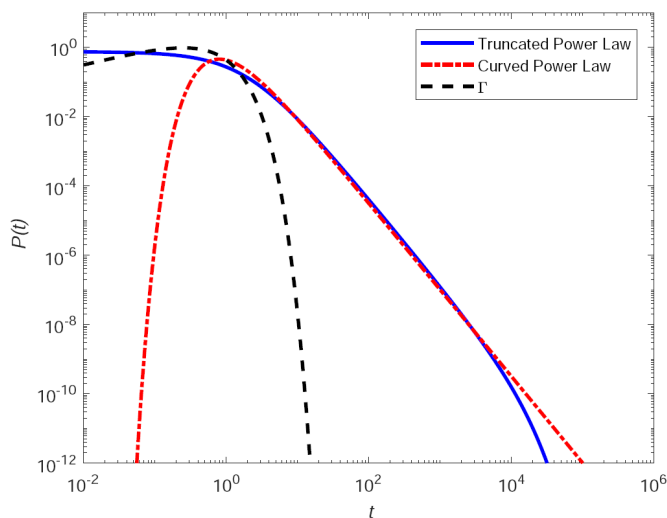
849 Indeed, let us compare the gamma distribution in the form of Eq. (8) to the inverse gamma
850 distribution as shown in Eq. (6). Aside from the normalisation coefficients, the inverse
851 gamma and gamma distributions shown in Eqs. (6) and (8) differ in two fundamental ways –
852 the power law (exponent of t) terms, $t^{-1-\beta}$ vs. $t^{-1+\beta}$ and the exponential terms, $\exp(-t^*/t)$ vs.



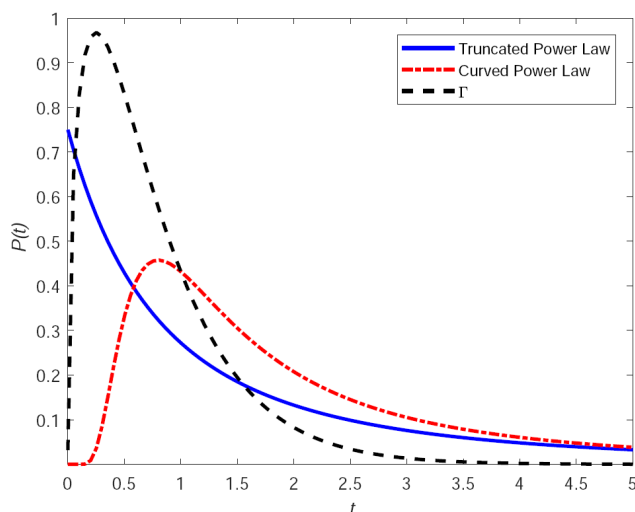
853 $\exp(-t/t^*)$, respectively. We stress again, as explained in Sect. 3.2, that the *inverse* gamma
854 distribution is a power law distribution (without an exponential cut-off time to allow transition
855 to Fickian transport), and thus one form of transition time distribution $\psi(t)$ in the CTRW
856 formulation.

857 We plot in Fig. 6a the truncated power law, curved power law (inverse gamma) and
858 gamma (transition time) distributions, $P(t)$, for the specific parameters $\beta = 1.5$, $t_1 = 1$, $t_2 = 10^3$,
859 $t^* = t_1$. We plot in log-log scale to emphasize the long-time portion of the transition time
860 distribution. Figure 6b shows the same curves plotted on a linear scale, to contrast the fact that
861 linear plots (noting the short time scale on the x -axis) do not illustrate the long-time
862 contributions, which can have a critical effect on the overall transport behaviour. Clearly,
863 from Fig. 6b, the gamma distribution does not include the possibility of long times; it has
864 an exponential cut-off to Gaussian behaviour at times larger than t^* , as the exponential term
865 dominates the power law term when $t \gg t^*$. However, note that the power law is $t^{-1+\beta}$ rather
866 than $t^{-1-\beta}$. The inverse gamma distribution, on the other hand, does not display an exponential
867 cut-off, but has the same $t^{-1-\beta}$ power law scaling as the TPL.

868 We thus conclude (recall also the conceptual picture and discussion in Sect. 3.1) that
869 although there is no universally “right” or “wrong” choice, the gamma distribution does not
870 generally appear as a suitable “candidate” to quantify chemical transport in surface water
871 systems, notwithstanding its empirical use in the literature. We suggest that the CTRW
872 framework (Sect. 3.3) rests on a more physically justified conceptual picture and
873 corresponding, coherent and robust mathematical formulation. The choice of a truncated
874 power law or inverse gamma distributions is largely a function of scale. The inverse gamma
875 distribution may better suit pore-scale (microscale) domains, where the peak of the function is
876 important, and where ergodicity is not relevant (the cut-off is not needed). Using the truncated
877 power law is “more” general, and better suits a variety of larger scale problems.
878



879 (a)



880

(b)

881 **Figure 6** Truncated power law, curved power law (inverse gamma distribution) and gamma
 882 distribution, for the specific parameters: $\beta = 1.5$, $t_1 = 1$, $t_2 = 10^3$, $t^* = t_1$. (a) Log-log scale to
 883 emphasise the long-time tailing behaviour. (b) Linear scale.

884

885 We now consider a specific example that demonstrates the relevance and applicability of
 886 the CTRW framework for chemical transport in surface water systems, keeping the above
 887 arguments in mind. Referring to the 2D case shown in Fig. 5a, we consider the effective
 888 response, $h(t)$, to a rainfall pulse containing a chemical species over the entire area of a
 889 catchment. Every point over this area may be considered a source of chemical species (“tracer”).
 890 A stream running through the catchment acts as a line sink (collector) for the tracer. This
 891 catchment picture can be idealised as two rectangles straddling this stream sink (Fig. 5a).
 892 Measurements of tracer arrivals at a control point downstream of this stream (known as an
 893 “absorbing boundary”) yield a tracer arrival “counting rate” that is a breakthrough curve.

894 The first-passage time distribution $F(\mathbf{l}_s, t)$ defines the travel time distribution from a
 895 (pulse) source at the origin \mathbf{l} to the point \mathbf{l}_s . Then the chemical tracer/species concentration at
 896 position \mathbf{l}_s and time t , $c_s(\mathbf{l}_s, t)$ is given by

897

$$c_s(\mathbf{l}_s, t) = \int_0^{\infty} \sum_{\mathbf{l} \in \Omega} F(\mathbf{l}_s - \mathbf{l}, t') c_R(\mathbf{l}, t - t') dt' \quad (9)$$

898

900 where $c_R(t; \mathbf{l})$ is the chemical input from rainfall at a position \mathbf{l} in a catchment of area Ω .
 901 Referring then to Fig. 5a, because we sample chemical arrivals downstream, we can consider
 902 the sampling position as an “instantaneous” integration of all chemical species/tracer arrivals
 903 from the catchment pathways along the entire length of the stream. Travel time within the
 904 stream can generally be assumed negligible, relative to the catchment travel times, as stream
 905 velocities are generally much faster than combined overland/subsurface flows. We thus
 906 determine the total chemical flux into the stream by integrating over all chemical inputs in the
 907 catchment that reach the stream; this defines overall first-passage time distributions at the
 908 downstream measurement point. Assuming that all of the sampling positions in \mathbf{l}_s are small



909 regions compared to Ω , then $c_s(\mathbf{l}_s, t) \approx c_s$. For uniform rainfall distribution over Ω , we have
910 $c_R(\mathbf{l}, t) \approx c_R(t)$, and we can hence define for the effective response

911
912
$$h(t) \equiv \sum_{\mathbf{l} \in \Omega} F(\mathbf{l}, t) . \quad (10)$$

913

914 Long-term measurements of chloride tracer concentrations $c_R(t)$ in the rainfall over a
915 catchment area in Plynlimon, Wales, were compared to the time series of the chloride tracer
916 concentration $c_s(t)$ in the catchment Hafren stream (Kirchner et al., 2000). These authors
917 related the input and output concentrations through the convolution integral

918
919
$$c_s(t) = \int_0^\infty h(t') c_R(t - t') dt' . \quad (11)$$

920

921 Using a spectral analysis, Kirchner et al. (2000) concluded that overall chloride transport in
922 the catchment scaled as $h(t) \sim t^{-m}$, with $m \approx 0.5$, over a time period from 0.01 to 10 years.
923 They reported similar scaling in North American and Scandinavian field sites with $m \approx 0.4$ –
924 0.65.

925 Kirchner et al. (2000) continued their analysis by noting (i) that an exponential travel time
926 distribution (which is implicit in the advection-dispersion equation; see discussion above Eq.
927 (5)) does not match the data, and (ii) that conceptualization of the entire catchment as a single
928 flow path, and use of the advection-dispersion equation to describe travel times, do not
929 correctly match even the basic character of the chloride concentration arrivals. The authors
930 concluded that catchment travel time distributions should be quantified as an approximate
931 power law distribution, to correctly account for long-time chemical retention and release in
932 catchments, and defined $h(t)$ as a gamma distribution (recall Eq. (8)).

933 Scher et al. (2002) reanalysed this catchment system behaviour with the CTRW
934 framework, arguing that subsurface flow and transport are dominant factors controlling the
935 overall chemical species arrival to the stream outlet measurement point. Based on Eqs. (9) and
936 (10), they first (re)examined the solution of the one-dimensional advection-dispersion
937 equation; they confirmed that the temporal dependence of $h(t)$ does not represent the field
938 measurements (similar to Kirchner et al., 2000). Significantly, though, they employed a pure
939 power law form of the transition time distribution, $\psi(t) \sim t^{-1-\beta}$, and developed Eqs. (9) and
940 (10) – based on the seminal analysis of Scher and Montroll (1975) – to obtain

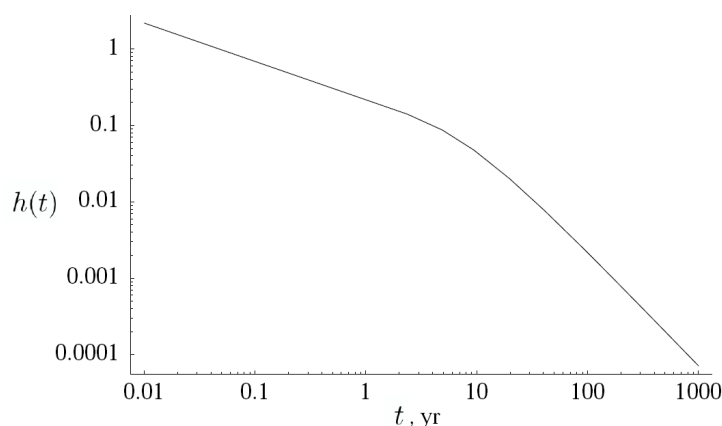
941
942
$$h(t) \sim \begin{cases} t^{-1+\beta}, & t < t^* \\ t^{-1-\beta}, & t > t^* \end{cases} . \quad (12)$$

943

944 The turnover time t^* between these two slopes arises naturally as an outcome of chemical
945 transport in the system embodied in Eq. (10). The smaller times represent chemical inputs
946 following along fastest flow paths to the sampling point; for $t > t^*$, all chemical inputs over
947 the entire catchment area are contributing particles to the sampling point, as accounted for in
948 Eq. (11). In this latter case, the power law represents the overall particle movement in the
949 domain, but especially the effects of the slow particles (longer transition times and influence
950 of less mobile zones) and the longer travel distances.



951 In the context of the Hafren stream system, the turnover time t^* was estimated as about 10
952 years (Scher et al., 2002), in agreement with findings and measurement range of Kirchner et
953 al. (2000), with $\beta = 1/2$. Figure 7 shows a representative plot of Eq. (12) for this system. As
954 noted in Scher et al. (2002), it remains to analyse measurements to confirm the turnover to the
955 longer-time $t^{-1-\beta}$ scaling behaviour, which is indicative of extremely long retention times.
956 Note that high-resolution measurements of concentration are generally required to analyse
957 these longer-time tails. The key recognition here is that while the effective catchment
958 response *may potentially*, initially (i.e. at relatively short times), be represented by a type of
959 gamma distribution (i.e., a power law $\sim t^{-1+\beta}$, ignoring the exponential cut-off) at sufficiently
960 small times (< 10 years in the case of the Hafren catchment) – and this is embodied in the
961 CTRW framework as seen in Eq. (12) – full (CTRW framework) power law behaviour (i.e.,
962 $\sim t^{-1-\beta}$) over longer times should also be incorporated to describe expected long-term
963 catchment retention behaviour. An evolution to Fickian transport, via an exponential cut-off at
964 very long times, can also be included (if relevant). To conclude, while direct, quantitative
965 application of CTRW to analysis of chemical transport at the catchment scale remains to be
966 done, it appears – on the basis of the conceptual pictures, extensive application to subsurface
967 systems and direct similarities to catchment systems, and the robust and general nature of the
968 CTRW formulation – to be a highly promising avenue for future research.
969



970
971 **Figure 7** A log-log plot of $h(t)$ vs. t (after Scher et al., 2002; Copyright 2002, with permission
972 from the American Geophysical Union).
973



974 **4 ADDITIONAL UNIFYING PERSPECTIVES ON PATTERNS AND**
975 **FUNCTIONING OF SURFACE WATER AND GROUNDWATER**
976 **SYSTEMS**

977 **4.1 Preferential flow and non-Gaussian travel times: The spatial and the**
978 **temporal manifestation of organized complexity**

979 Based on Sects. 2 and 3, we can state that (a) preferential flow and related non-Fickian
980 transport is an omnipresent, unifying element between both water worlds, and (b) the CTRW
981 framework can effectively quantify and predict non-Gaussian residence times of water and
982 chemicals species, in a manner that connects to and clearly steps beyond the advection-
983 dispersion paradigm. In this section, we link these insights to our central proposition that
984 preferential flow is a prime manifestation of how a local-scale heterogeneous flow process
985 causes a macroscale organised flow pattern in *space*. The key is to acknowledge that
986 organisation manifests also through organised dynamic behaviour in *time*, which occurs
987 through non-Gaussian travel time distributions of water and chemical species. Note that the
988 degree of organisation in *space* manifests in the deviation of spatial patterns of system
989 characteristics or fluid flow from the maximum entropy pattern. The latter corresponds, in the
990 case that the mean value is known, to a uniform distribution of system characteristics and/or a
991 uniform flow pattern. Along the same lines, we propose that the degree of organisation in
992 dynamic behaviour in *time* manifests through the deviation of the breakthrough curve from
993 the case of a well-mixed Gaussian system, which is quantified within the CTRW framework
994 based on the power law exponent. A power law exponent ≥ 2 corresponds to Gaussian
995 residence time distribution, and the latter maximises entropy when the *mean* and the *variance*
996 are known.

997 **4.2 Connecting the energy and travel time perspectives on preferential fluid**
998 **flow**

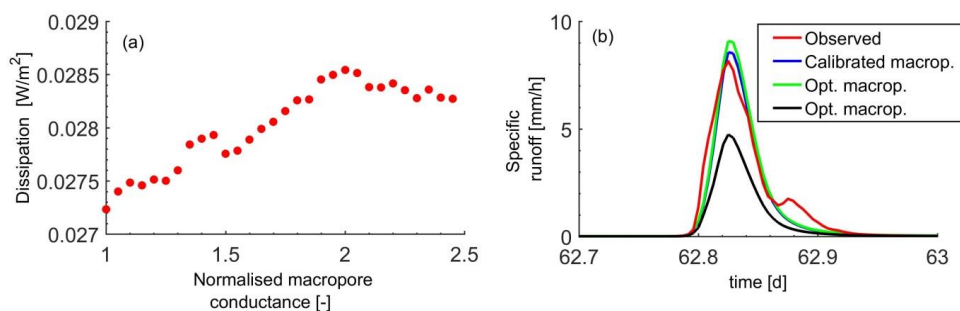
999 At this stage, we propose to connect travel time and energy perspectives on preferential
1000 fluid flow. This is, first, because the energy perspective provides a common framework for
1001 explaining why preferential flow phenomena occur. Preferential flow leads to faster fluid
1002 flows, because they reduce dissipative losses due to an increased hydraulic radius in the rill or
1003 river network compared to sheet to overland flow in surface water systems. Subsurface
1004 preferential flow of water reduces dissipative losses as well, as friction occurs mainly at
1005 macropore or fracture walls, while frictional interactions in the matrix occur along the entire
1006 inner surface. Reduced dissipation and faster fluid flow imply a more energy efficient
1007 throughput of water, mass and chemical species through the entire system (in case of flow
1008 paths spanning the entire system). While this increased energy efficiency is, at first sight, a
1009 purely diagnostic observation, it explains the growth phase of rill and river networks, and why
1010 they grow in a *directed* fashion. This is because flow against the gradient implies higher
1011 stream power, defined as volumetric flow times the geopotential gradient, which means that
1012 more kinetic energy can be transferred to the sediments. The related higher erosion rates
1013 imply an upslope growth of, for instance, a rill network (Paik and Kumar, 2010; Kleidon et al.
1014 2013).



1015 A faster flow against the driving gradient means that the latter becomes depleted more
1016 rapidly, which in turn means that entropy is produced. This slow negative feedback works
1017 against structural growth of rills and river network (Kleidon et al. 2013), and in open systems
1018 this implies the existence of metastable thermodynamic optimal states. Pioneering work in
1019 this respect by Paltridge (1979) successfully modelled planetary heat transport with a simple
1020 box model, assuming a steady state that maximised entropy production. Even earlier, Howard
1021 (1971, cited in Howard 1990) proposed that angles of river junctions are arranged in such way
1022 that they minimize stream power; later he expanded this to the idea that the topology of river
1023 networks reflects an energetic optimum, formulated as a minimum in total dissipation in the
1024 network (Howard, 1990). This was developed further by Rinaldo et al. (1996) as a concept of
1025 minimum energy expenditure.

1026 Hergarten et al. (2014) transferred this idea to groundwater systems by analysing
1027 preferential flow paths that minimise the total energy dissipation at a given recharge, under
1028 the constraint of a given total porosity and by verifying against data sets for spring discharge
1029 in the Austrian Alps. Minimum energy expenditure in the river network implies that power,
1030 i.e., kinetic energy flux through the system, is maximised. In this light, Kleidon et al. (2013)
1031 showed that directed structural growth in the topology of connected river networks can be
1032 explained through a maximisation of kinetic energy transfer to sediment flows. Zehe et al.
1033 (2013) expressed the total soil water potential to its free energy, and analysed free energy
1034 changes associated with soil water dynamics within a physically based model study based on
1035 the extensive Weiherbach data set. These authors varied the density of preferential flow paths
1036 in the partially saturated soil within a range from zero up to a density, where their
1037 conductance was 2.5 times the saturated hydraulic conductivity of the soil matrix. Within this
1038 range, they found two optima that maximized the averaged entropy production during
1039 recharge events. One of these optima allowed an acceptable prediction of the rainfall runoff
1040 response of the Weiherbach without any calibration to discharge data (Fig. 8).

1041



1042

1043

1044 **Figure 8 (a)** Total dissipation of free energy of soil water as function of the normalised
1045 macropore conductance. The latter is total hydraulic conductivity summed of all macropores
1046 in the model domain divided to the saturated hydraulic conductivity of the soil matrix. **(b)**
1047 Simulated specific runoff with a macroporosity calibrated to match discharge response of the
1048 catchment (Calibrated macrop.), uncalibrated simulations based on the two local optima
1049 macroporosities (Opt. macrop.) and observed specific discharge at the catchment outlet (after
1050 Zehe et al., 2013).



1051

1052

1053

1054

1055

1056

1057

1058

1059

1060

1061

1062

1063

1064

1065

1066

1067

1068

So – do hydrological systems, their storage capacity and particularly preferential flow networks therein, evolve to metastable states in accordance with thermodynamic optimality (Zehe et al., 2019; Savenije and Hrachowitz, 2017), or at least towards a more energy efficient throughput of water, chemical species and mass flow through the system? While the above mentioned studies might be interpreted this way, other studies speak against this idea (Westhoff and Zehe, 2013). The question as to whether thermodynamic optimality should thus be seen as more than a sometimes helpful constraint is far from being solved (Westhoff et al., 2019). Here, the travel time perspective and CTRW come into play, because they offer an avenue to diagnose whether a system is or is not in such an optimality state. This can be done through optimising models representing hydrological systems of interest, including their preferential flow network, such that they function in accordance with an optimality principle, e.g. MEP as outlined above. One can then simulate tracer transport through these optimised system as, e.g., shown in Fig. 3, analyse the breakthrough curve with CTRW, and compare the outcome to corresponding tracer test performed in the real system. The matching of breakthrough curves within the uncertainty range suggests a generic test that can shed light on this controversial question, whether self-organisation in open hydrological systems leads to an evolution to a more energy efficient or even optimal system configuration, or not.

1069

5 CONCLUSIONS AND PERSPECTIVES

1070

1071

1072

1073

1074

1075

1076

1077

1078

In an effort to integrate and unify conceptualisation and quantitative modelling of the two “water worlds” – surface water and groundwater systems – we recognise preferential fluid flows as a unifying element and consider them as a manifestation of self-organisation. Preferential flows hinder perfect mixing within a system, due to a more “energy efficient” and hence faster throughput of water, which affects residence times of water, matter and chemical species in hydrological systems across all scales. While our main focus here is on the role of preferential flow for residence times and chemical transport, we relate our proposed unifying concept to role of preferential flow for energy conversions and energy dissipation associated with flows of water and mass.

1079

1080

1081

1082

1083

1084

1085

1086

1087

1088

1089

1090

1091

1092

Essentially, we have proposed that related conceptualisations on the role of heterogeneity and preferential fluid flow for chemical species transport, and its quantitative characterisation, can be unified in terms of a theory, based on the CTRW framework, that connects these two water worlds in a dynamic framework. We emphasise the occurrence of power law behaviours that characterise travel times of chemical species, and highlight the critical role played by system heterogeneity and chemical species residence times, which are distinct from travel times of water. In particular, we compare and contrast specific power law distributions, and argue that the closely related inverse gamma and algebraic power law distributions are more appropriate than the oft-used gamma distribution to quantify chemical species transport.

Moreover, we identify deviations from well-mixed Gaussian transport as a manifestation of self-organised dynamic behaviour in time, and the power law exponent as a suitable means to measure the strength of this deviation. Along a complementary line, we propose that self-organisation in space is immanent primarily through strongly localised preferential flow through rill and river networks at the land surface. We relate the degree of spatial organisation



1093 to the deviation of the flow pattern from spatially homogeneous flow, which is a state of
1094 maximum entropy. In this context, we reflect on the ongoing controversial discussion
1095 regarding whether or not self-organisation in open hydrological systems leads to evolution to
1096 a more energy efficient or even thermodynamic optimal system configuration. Finally, we
1097 propose that our concept of temporally organised travel times can help to test the possible
1098 emergence of thermodynamic optimality. Complementary to this idea, we suggest that an
1099 energetic perspective of chemical species transport may help to explain the organisation of
1100 travel paths (Fig. 3), in the sense that contrary to common assumptions, preferential pathways
1101 often include “bottlenecks” of low hydraulic conductivity. A testable option could be that
1102 chemical species travel along the path of maximum power, with power being defined in this
1103 case as flow of chemical energy (rather than flow of kinetic energy) through the system.

1104 Overall, we conclude that self-organisation arises equally in surface water and
1105 groundwater systems, as local heterogeneity and disorder in fluid flow and chemical transport
1106 processes lead to ordered behaviour at the macroscale. Naturally, the surface water
1107 community has developed a strong emphasis on the *localised spatial fingerprints*, because
1108 rills and rivers are clearly visible on land (Fig. 1), while the groundwater community has
1109 focused more naturally on *non-local temporal fingerprints*, as the flow paths are largely
1110 unobservable. But these are just two sides of the same conceptual picture of organised
1111 complexity (Dooge, 1986).

1112

1113 **Competing interests.** The authors declare that they have no conflict of interest.

1114

1115 **Acknowledgements.** B.B. gratefully acknowledges the support of research grants from the
1116 Israel Water Authority (Grant No. 45015199895) and the Israel Science Foundation (Grant
1117 No. 485/16); he thanks Harvey Scher for in-depth discussions. B.B. holds the Sam Zuckerberg
1118 Professorial Chair in Hydrology. E.Z. gratefully acknowledges intellectual support by the
1119 “Catchments as Organized Systems” (CAOS) research unit and funding of the German
1120 Research Foundation, DFG, (FOR 1598, ZE 533/11-1, ZE 533/12-1).

1121

1122 6 REFERENCES

- 1123 Abramowitz, M. and Stegun, I.: Handbook of Mathematical Functions, Dover, Mineola, N.Y.,
1124 1970.
- 1125 Angermann, L., Jackisch, C., Allroggen, N., Sprenger, M., Zehe, E., Tronicke, J., Weiler, M.,
1126 and Blume, T.: Form and function in hillslope hydrology: Characterization of subsurface
1127 flow based on response observations, Hydrology And Earth System Sciences, 21, 3727-
1128 3748, doi:10.5194/hess-21-3727-2017, 2017.
- 1129 Aronofsky, J. S. and Heller, J. P.: A diffusion model to explain mixing of flowing miscible
1130 fluids in porous media, Trans. Am. Inst. Min. Metall. Pet. Eng., 210, 345-349, 1957.
- 1131 Bardossy, A.: Copula-based geostatistical models for groundwater quality parameters, Water
1132 Resour. Res., 42, W11416, doi:10.1029/2005wr004754, 2006.
- 1133 Bardossy, A.: Calibration of hydrological model parameters for ungauged catchments,
1134 Hydrol. Earth Syst. Sci., 11, 703-710, doi:10.5194/hess-11-703-2007, 2007.



- 1135 Bardossy, A. and Singh, S. K.: Robust estimation of hydrological model parameters, *Hydrol.*
1136 *Earth Syst. Sci.*, 12, 1273-1283, doi:10.5194/hess-12-1273-2008, 2008.
- 1137 Bejan, A., Lorente, S., and Lee, J.: Unifying constructal theory of tree roots, canopies and
1138 forests, *J. Theor. Biol.*, 254, 529-540, doi:10.1016/j.jtbi.2008.06.026, 2008.
- 1139 Benettin, P., and Bertuzzo, E.: Tran-sas v1.0: A numerical model to compute catchment-scale
1140 hydrologic transport using storage selection functions, *Geosci. Model Devel.*, 11, 1627-
1141 1639, doi:10.5194/gmd-11-1627-2018, 2018.
- 1142 Benettin, P., Volkmann, T. H. M., von Freyberg, J., Frentress, J., Penna, D., Dawson, T. E.,
1143 and Kirchner, J.: Effects of climatic seasonality on the isotopic composition of evaporating
1144 soil waters, *Hydrol. Earth Syst. Sci.*, 22, 2881-2890, doi:10.5194/hess-22-2881-2018,
1145 2018.
- 1146 Ben-Zvi, R., Jiang, S., Scher, H., and Berkowitz, B.: Finite-Element Method solution of non-
1147 Fickian transport in porous media: The CTRW-FEM package, *Groundwater*, 57, 479-484,
1148 doi:10.1111/gwat.12813, 2019.
- 1149 Berkowitz, B. and Scher, H.: Exploring the nature of non-Fickian transport in laboratory
1150 experiments, *Adv. Water Resour.*, 32, 750-755, doi:10.1016/j.advwatres.2008.05.004,
1151 2009.
- 1152 Berkowitz, B., Cortis, A., Dentz, M., and Scher, H.: Modeling non-Fickian transport in
1153 geological formations as a continuous time random walk, *Rev. Geophys.*, 44, RG2003,
1154 doi:10.1029/2005RG000178, 2006.
- 1155 Berkowitz, B., Dror, I., Hansen, S. K., and Scher, H.: Measurements and models of reactive
1156 transport in geological media, *Rev. Geophys.*, 54, 930-986, doi:10.1002/2016RG000524,
1157 2016.
- 1158 Beven, K.: Changing ideas in hydrology - the case of physically-based models, *J. Hydrol.*,
1159 105, 157-172, doi:10.1016/0022-1694(89)90101-7, 1989.
- 1160 Beven, J. K. and Binley, A.: The future of distributed models: Model calibration and
1161 uncertainty prediction, *Hydrol. Proc.*, 6, 265-277, doi:10.1002/hyp.3360060305, 1992.
- 1162 Beven, K. and Germann, K.: Macropores and water flow in soils, *Water Resour. Res.*, 18,
1163 1311-1325, doi:10.1029/WR018i005p01311, 1982.
- 1164 Beven, K. and Germann, P.: Macropores and water flow in soils revisited, *Water Resour.*
1165 *Res.*, 49, 3071-3092, doi:10.1002/wrcr.20156, 2013.
- 1166 Bianchi, M., Zheng, C., Wilson, C., Tick, G. R., Liu, G., and Gorelick, S. M.: Spatial
1167 connectivity in a highly heterogeneous aquifer: From cores to preferential flow paths,
1168 *Water Resour. Res.*, 47, W05524, doi:10.1029/2009WR008966, 2011.
- 1169 Binet, F., Kersante, A., Munier-Lamy, C., Le Bayon, R. C., Belgy, M. J., and Shipitalo, M. J.:
1170 Lumbricid macrofauna alter atrazine mineralization and sorption in a silt loam soil, *Soil*
1171 *Biol. Biochem.*, 38, 1255-1263, doi:10.1016/j.soilbio.2005.09.018, 2006.
- 1172 Binley, A. and Beven, K. J.: Vadose zone model uncertainty as conditioned on geophysical
1173 data, *Ground Water*, 41, 119-127, doi:10.1111/j.1745-6584.2003.tb02576.x, 2003.
- 1174 Blume, T., Zehe, E., and Bronstert, A.: Investigation of runoff generation in a pristine, poorly
1175 gauged catchment in the Chilean Andes II: Qualitative and quantitative use of tracers at
1176 three spatial scales, *Hydrol. Proc.*, 22, 3676-3688, doi:10.1002/hyp.6970, 2008.



- 1177 Blume, T., Zehe, E., and Bronstert, A.: Use of soil moisture dynamics and patterns at different
1178 spatio-temporal scales for the investigation of subsurface flow processes, *Hydrol. Earth*
1179 *Syst. Sci.* 13, 1215-1233, doi:10.5194/hess-13-1215-2009, 2009.
- 1180 Boano, F., Packman, A.I., Cortis, A., Revelli, R., and Ridolfi, L.: A continuous time random
1181 walk approach to the stream transport of solutes, *Water Resour. Res.*, 43, W10425,
1182 doi:10.1029/2007WR006062, 2007.
- 1183 Bolduan, R. and Zehe, E.: Degradation of isoproturon in earthworm macropores and subsoil
1184 matrix - a field study, *J. Plant Nutrition Soil Sci.*, 169, 87-94, doi:10.1002/jpin.200521754,
1185 2006.
- 1186 Bonell, M., Pearce, A. J., and Stewart, M. K.: The identification of runoff-production
1187 mechanisms using environmental isotopes in a tussock grassland catchment, eastern otago,
1188 new-zealand, *Hydrol. Proc.*, 4, 15-34, doi:10.1002/hyp.3360040103, 1990.
- 1189 Botter G., Bertuzzo E., and Rinaldo A.: Transport in the hydrologic response: Travel time
1190 distributions, soil moisture dynamics, and the old water paradox, *Water Resour. Res.*,
1191 46(3), W03514, doi:10.1029/2009WR008371, 2010.
- 1192 Botter G., Bertuzzo E., and Rinaldo A.: Catchment residence and travel time distributions:
1193 The master equation, *Geophys. Res. Lett.*, 38(11), L11403, doi:10.1029/2011GL047666,
1194 2011.
- 1195 Brooks, J. R., Barnard, H. R., Coulombe, R., and McDonnell, J. J.: Ecohydrologic separation
1196 of water between trees and streams in a mediterranean climate, *Nature Geosci.*, 3, 100-104,
1197 doi:10.1038/ngeo722, 2010.
- 1198 Bundt, M., Widmer, F., Pesaro, M., Zeyer, J., and Blaser, P.: Preferential flow paths:
1199 Biological 'hot spots' in soils, *Soil Biol. Biochem.*, 33, 729-738, doi:10.1016/S0038-
1200 0717(00)00218-2, 2001.
- 1201 Camporese, M., Paniconi, C., Putti, M., and Orlandini, S.: Surface-subsurface flow modeling
1202 with path-based runoff routing, boundary condition-based coupling, and assimilation of
1203 multisource observation data, *Water Resour. Res.*, 46, W0251210,
1204 doi:1029/2008wr007536, 2010.
- 1205 Chabrier, G., Galactic stellar and substellar initial mass function, *Publ. Astron. Soc. Pac.* 115,
1206 763-795, doi:10.1086/376392, 2003.
- 1207 Collins, R., Jenkins, A., and Harrow, M. A.: The contribution of old and new water to a storm
1208 hydrograph determined by tracer addition to a whole catchment, *Hydrol. Processes*, 14,
1209 701-711. doi:10.1002/(SICI)1099-1085(200003)14:43.0.CO;2-2, 2000.
- 1210 Cortis A. and Berkowitz B.: Computing "anomalous" contaminant transport in porous media:
1211 The CTRW MATLAB toolbox, *Ground Water*, 43, 947-950, doi:10.1111/j.1745-
1212 6584.2005.00045.x, 2005.
- 1213 Davies, J. and Beven, K.: Comparison of a multiple interacting pathways model with a
1214 classical kinematic wave subsurface flow solution, *Hydrol. Sci. J.-J. Sci. Hydrol.*, 57, 203-
1215 216, doi:10.1080/02626667.2011.645476, 2012.
- 1216 Davies, J., Beven, K., Rodhe, A., Nyberg, L., and Bishop, K.: Integrated modeling of flow
1217 and residence times at the catchment scale with multiple interacting pathways, *Water*
1218 *Resour. Res.*, 49, 4738-4750, doi:10.1002/wrcr.20377, 2013.



- 1219 Dentz, M., Scher, H., Holder, D., and Berkowitz, B.: Transport behaviour of coupled
1220 continuous-time random walks, *Phys. Rev. E*, 78, 41110,
1221 doi:10.1103/PhysRevE.78.041110, 2008.
- 1222 Dooge, J. C. I.: Looking for hydrological laws, *Water Resour. Res.*, 22, 46S-58S,
1223 doi:10.1029/WR022i09Sp0046S, 1986.
- 1224 Duan, Q. Y., Sorooshian, S., and Gupta, H. V.: Effective and efficient global optimization for
1225 conceptual rainfall-runoff models, *Water Resour. Res.*, 28, 1015-1031,
1226 doi:10.1029/91WR02985, 1992.
- 1227 Edery, Y., Guadagnini, A., Scher, H., and Berkowitz, B.: Origins of anomalous transport in
1228 disordered media: Structural and dynamic controls, *Water Resour. Res.*, 50, 1490-1505,
1229 doi:10.1002/2013WR015111, 2014.
- 1230 Evaristo, J., Jasechko, S., and McDonnell, J. J.: Global separation of plant transpiration from
1231 groundwater and streamflow, *Nature*, 525, 91-94, doi:10.1038/nature14983, 2015.
- 1232 Everett, M. E.: *Near-Surface Applied Geophysics*, Cambridge University Press, Cambridge,
1233 2013.
- 1234 Ewen, J.: 'Samp' model for water and solute movement in unsaturated porous media involving
1235 thermodynamic subsystems and moving packets 1. Theory, *J. Hydrol.*, 182, 175-194,
1236 doi:10.1016/0022-1694(95)02925-7, 1996a.
- 1237 Ewen, J.: 'Samp' model for water and solute movement in unsaturated porous media involving
1238 thermodynamic subsystems and moving packets 2. Design and application, *J. Hydrol.*, 182,
1239 195-207, doi:10.1016/0022-1694(95)02926-5, 1996b.
- 1240 Faulkner, H.: Connectivity as a crucial determinant of badland morphology and evolution,
1241 *Geomorphology*, 100, 91-103, doi:10.1016/j.geomorph.2007.04.039, 2008.
- 1242 Fenicia, F., Kavetski, D., and Savenije, H. H. G.: Elements of a flexible approach for
1243 conceptual hydrological modeling: 1. Motivation and theoretical development, *Water*
1244 *Resour. Res.*, 47, W11510, doi:10.1029/2010wr010174, 2011.
- 1245 Fenicia, F., Kavetski, D., Savenije, H. H. G., Clark, M. P., Schoups, G., Pfister, L., and Freer,
1246 J.: Catchment properties, function, and conceptual model representation: Is there a
1247 correspondence?, *Hydrol. Proc.*, 28, 2451-2467, doi:10.1002/hyp.9726, 2014.
- 1248 Feyen, L., Vazquez, R., Christiaens, K., Sels, O., and Feyen, J.: Application of a distributed
1249 physically-based hydrological model to a medium size catchment, *Hydrol. Earth Syst. Sci.*,
1250 4, 47-63, doi:10.5194/hess-4-47-2000, 2000.
- 1251 Flury, M.: Experimental evidence of transport of pesticides through field soils - a review, *J.*
1252 *Environ. Qual.*, 25, 25-45, doi:10.2134/jeq1996.00472425002500010005x, 1996.
- 1253 Flury, M., Flühler, H., Leuenberger, J., and Jury, W. A.: Susceptibility of soils to preferential
1254 flow of water: A field study, *Water Resour. Res.*, 30, 1945-1954,
1255 doi:10.1029/94WR00871, 1994.
- 1256 Flury, M., Leuenberger, J., Studer, B., and Flühler, H.: Transport of anions and herbicides in a
1257 loamy and a sandy soil. , *Water Resour. Res.*, 31, 823-835, doi:10.1029/94WR02852,
1258 1995.
- 1259 Freeze, R. A. and Harlan, R. L.: Blueprint for a physically-based, digitally simulated
1260 hydrologic response model, *J. Hydrol.*, 9, 237-258, doi:10.1016/0022-1694(69)90020-1,
1261 1969.



- 1262 Gao, H., Hrachowitz, M., Fenicia, F., Gharari, S., and Savenije, H. H. G.: Testing the realism
1263 of a topography-driven model (flex-topo) in the nested catchments of the Upper Heihe,
1264 China, *Hydrol. Earth Syst. Sci.*, 18, 1895-1915, doi:10.5194/hess-18-1895-2014, 2014.
- 1265 Gärdenäs, A. I., Šimunek, J., Jarvis, N., and van Genuchten, M. T.: Two-dimensional
1266 modelling of preferential water flow and pesticide transport from a tile-drained field, *J.*
1267 *Hydrol.*, 329, 647-660, doi:10.1016/j.jhydrol.2006.03.021, 2006.
- 1268 Gassmann, M., Stamm, C., Olsson, O., Lange, J., Kümmerer, K., and Weiler, M.: Model-
1269 based estimation of pesticides and transformation products and their export pathways in a
1270 headwater catchment, *Hydrol. Earth Syst. Sci.*, 17, 5213-5228, doi:10.5194/hess-17-5213-
1271 2013, 2013.
- 1272 Gharari, S., Hrachowitz, M., Fenicia, F., and Savenije, H. H. G.: Hydrological landscape
1273 classification: Investigating the performance of hand based landscape classifications in a
1274 central european meso-scale catchment, *Hydrol. Earth Syst. Sci.*, 15, 3275-3291,
1275 doi:10.5194/hess-15-3275-2011, 2011.
- 1276 Goldstein, H.: *Classical Mechanics*, Pearson Education Limited, Harlow, U.K., 2013.
- 1277 Goller, R., Wilcke, W., Fleischbein, K., Valarezo, C., and Zech, W.: Dissolved nitrogen,
1278 phosphorus, and sulfur forms in the ecosystem fluxes of a montane forest in Ecuador.
1279 *Biogeochemistry*, 77, 57-89, doi:10.1007/s10533-005-1061-1, 2006.
- 1280 Gooseff, M. N., Wondzell, S. M., Haggerty, R., and Anderson, J.: Comparing transient
1281 storage modeling and residence time distribution (RTD) analysis in geomorphically varied
1282 reaches in the Lookout Creek basin, Oregon, USA, *Adv. Water Resour.*, 26(9), 925-937,
1283 doi:10.1016/S0309-1708(03)00105-2, 2003.
- 1284 Gouet-Kaplan, M. and Berkowitz, B.: Measurements of interactions between resident and
1285 infiltrating water in a lattice micromodel, *Vadose Zone J.*, 10, 624-633,
1286 doi:10.2136/vzj2010.0103, 2011.
- 1287 Haggerty, R. and Gorelick S. M.: Multiple rate mass transfer for modeling diffusion and
1288 surface reactions in media with pore-scale heterogeneity, *Water Resour. Res.*, 31(10),
1289 2383-2400, doi:10.1029/95WR10583, 1995.
- 1290 Haggerty, R., Wondzell, S. M., and Johnson, M. A.: Power-law residence time distribution in
1291 the hyporheic zone of a 2nd-order mountain stream, *Geophys. Res. Lett.*, 29(13), 18-1-18-
1292 4, doi:10.1029/2002GL014743, 2002.
- 1293 Haken, H.: *Synergetics: An introduction; nonequilibrium phase transitions and self-*
1294 *organization in physics, chemistry and biology*, Springer Series in Synergetics, Springer
1295 Berlin, 355 pp., 1983.
- 1296 Hammel, K. and Roth, K.: Approximation of asymptotic dispersivity of conservative solute in
1297 unsaturated heterogeneous media with steady state flow, *Water Resour. Res.*, 34, 709-715,
1298 doi:10.1029/98WR00004, 1998.
- 1299 Harman, C. J.: Time-variable transit time distributions and transport: Theory and application
1300 to storage-dependent transport of chloride in a watershed, *Water Resour. Res.*, 51, 1-30,
1301 doi:10.1002/2014wr015707, 2015.
- 1302 He, Y., Bardossy, A., and Zehe, E.: A review of regionalisation for continuous streamflow
1303 simulation, *Hydrol. Earth Syst. Sci.*, 15, 3539-3553, doi:10.5194/hess-15-3539-2011,
1304 2011a.



- 1305 He, Y., Bardossy, A., and Zehe, E.: A catchment classification scheme using local variance
1306 reduction method, *J. Hydrol.*, 411, 140-154, doi:10.1016/j.jhydrol.2011.09.042, 2011b.
- 1307 Heidbuchel, I., Troch, P. A., and Lyon, S. W.: Separating physical and meteorological
1308 controls of variable transit times in zero-order catchments, *Water Resour. Res.*, 49, 7644-
1309 7657, doi:10.1002/2012wr013149, 2013.
- 1310 Hergarten, S., Winkler, G., and Birk, S.: Transferring the concept of minimum energy
1311 dissipation from river networks to subsurface flow patterns, *Hydrol. Earth Syst. Sci.*, 18,
1312 4277-4288, doi:10.5194/hess-18-4277-2014, 2014.
- 1313 Hildebrandt, A., Kleidon, A., and Bechmann, M.: A thermodynamic formulation of root water
1314 uptake, *Hydrol. Earth Syst. Sci.*, 20, 3441-3454, doi:10.5194/hess-20-3441-2016, 2016.
- 1315 Hoffman, F., Ronen, D., Pearl, Z.: Evaluation of flow characteristics of a sand column using
1316 magnetic resonance imaging, *J. Contam. Hydrol.*, 22, 95-107, doi:10.1016/0169-
1317 7722(95)00079-8, 1996.
- 1318 Howard, A. D.: Optimal angles of stream junctions: geometric stability to capture and
1319 minimum power criteria, *Water Resour. Res.*, 7, 863-873, doi:10.1029/WR007i004p00863,
1320 1971.
- 1321 Howard, A. D.: Theoretical model of optimal drainage networks, *Water Resour. Res.*, 26,
1322 2107-2117, doi:10.1029/WR026i009p02107, 1990.
- 1323 Hrachowitz, M., Savenije, H., Boogard, T. A., Tetzlaff, D., and Soulsby, C.: What can flux
1324 tracking teach us about water age distribution patterns and their temporal dynamics?,
1325 *Hydrol. Earth Syst. Sciences*, 17, 533-564, doi:10.5194/hess-17-533-2013, 2013.
- 1326 Hrachowitz, M., Soulsby, C., Tetzlaff, D., Malcolm, I. A., and Schoups, G.: Gamma
1327 distribution models for transit time estimation in catchments: Physical interpretation of
1328 parameters and implications for time-variant transit time assessment, *Water Resour. Res.*,
1329 46, W10536, doi:10.1029/2010WR009148, 2010.
- 1330 Hundecha, Y. and Bardossy, A.: Modeling of the effect of land use changes on the runoff
1331 generation of a river basin through parameter regionalization of a watershed model, *J.*
1332 *Hydrol.*, 292, 281-295, doi:10.1016/j.jhydrol.2004.01.002, 2004.
- 1333 Jackisch, C. and Zehe, E.: Ecohydrological particle model based on representative domains,
1334 *Hydrol. Earth Syst. Sci.*, 22, 3639-3662, doi:10.5194/hess-22-3639-2018, 2018.
- 1335 Jing, M., Heße, F., Kumar, R., Kolditz, O., Kalbacher, T., and Attinger, S.: Influence of input
1336 and parameter uncertainty on the prediction of catchment-scale groundwater travel time
1337 distributions, *Hydrol. Earth Syst. Sci.*, 23, 171-190, doi:10.5194/hess-23-171-2019, 2019.
- 1338 Kapetas, L., Dror, I., and Berkowitz, B.: Evidence of preferential path formation and path
1339 memory effect during successive infiltration and drainage cycles in uniform sand columns,
1340 *J. Contam. Hydrol.*, 165, 1-10, doi:10.1016/j.jconhyd.2014.06.016., 2014.
- 1341 Kirchner, J. W.: A double paradox in catchment hydrology and geochemistry, *Hydrol. Proc.*,
1342 17, 871-874, doi: 10.1002/hyp.5108, 2003.
- 1343 Kirchner, J. W.: Getting the right answers for the right reasons: Linking measurements,
1344 analyses, and models to advance the science of hydrology, *Water Resour. Res.*, 42,
1345 W03S04, doi:10.1029/2005wr004362, 2006.
- 1346 Kirchner, J. W.: Aggregation in environmental systems – Part 1: Seasonal tracer cycles
1347 quantify young water fractions, but not mean transit times, in spatially heterogeneous
1348 catchments, *Hydrol. Earth Syst. Sciences*, 279-297, doi:10.5194/hess-20-279-2016, 2016.



- 1349 Kirchner, J. W., Feng, X., and Neal, C.: Fractal stream chemistry and its implications for
1350 contaminant transport in catchments, *Nature*, 403, 524-527, doi:10.1038/35000537, 2000.
- 1351 Klaus, J. and Zehe, E.: Modelling rapid flow response of a tile drained field site using a 2D-
1352 physically based model: Assessment of “equifinal” model setups, *Hydrol. Proc.*, 24, 1595-
1353 1609, doi:10.1002/hyp.7687, 2010.
- 1354 Klaus, J. and Zehe, E.: A novel explicit approach to model bromide and pesticide transport in
1355 connected soil structures, *Hydrol. Earth Syst. Sci.*, 15, 2127-2144, doi:10.5194/hess-15-
1356 2127-2011, 2011.
- 1357 Klaus, J., Zehe, E., Elsner, M., Kulls, C., and McDonnell, J. J.: Macropore flow of old water
1358 revisited: Experimental insights from a tile-drained hillslope, *Hydrol. Earth Syst. Sci.*, 17,
1359 103-118, doi:10.5194/hess-17-103-2013, 2013.
- 1360 Klaus, J., Zehe, E., Elsner, M., Palm, J., Schneider, D., Schroeder, B., Steinbeiss, S., van
1361 Schaik, L., and West, S.: Controls of event-based pesticide leaching in natural soils: A
1362 systematic study based on replicated field scale irrigation experiments, *J. Hydrol.*, 512,
1363 528-539, doi:10.1016/j.jhydrol.2014.03.020, 2014.
- 1364 Klaus, J., Chun, K. P., McGuire, K. J., and McDonnell, J. J.: Temporal dynamics of
1365 catchment transit times from stable isotope data, *Water Resour. Res.*, 51, 4208-4223,
1366 doi:10.1002/2014wr016247, 2015.
- 1367 Kleidon, A.: How does the earth system generate and maintain thermodynamic disequilibrium
1368 and what does it imply for the future of the planet?, *Philos. Trans. Royal Soc. A-Math.*
1369 *Phys. Eng. Sci.*, 370, 1012-1040, doi:10.1098/rsta.2011.0316, 2012a.
- 1370 Kleidon, A., Zehe, E., and Lin, H.: Thermodynamic limits of the critical zone and their
1371 relevance to hydrogeology, in: *Hydrogeology: Synergistic Integration of Soil Science*
1372 *and Hydrology*, 5 Elsevier, Amsterdam, 854 pp., p. 243, 2012b.
- 1373 Kleidon, A., Zehe, E., Ehret, U., and Scherer, U.: Thermodynamics, maximum power, and the
1374 dynamics of preferential river flow structures at the continental scale, *Hydrol. Earth Syst.*
1375 *Sci.*, 17, 225-251, doi:10.5194/hess-17-225-2013, 2013.
- 1376 Kondepudi, D., and Prigogine, I.: *Modern thermodynamics: From heat engines to dissipative*
1377 *structures*, John Wiley Chichester, U.K., 1998.
- 1378 Lehmann, P., Hinz, C., McGrath, G., Tromp-van Meerveld, H. J., and McDonnell, J. J.:
1379 Rainfall threshold for hillslope outflow: An emergent property of flow pathway
1380 connectivity, *Hydrol. Earth Syst. Sci.*, 11, 1047-1063, doi:10.5194/hess-11-1047-2007,
1381 2007.
- 1382 Levy, M. and Berkowitz, B.: Measurement and analysis of non-Fickian dispersion in
1383 heterogeneous porous media, *J. Contam. Hydrol.*, 64(3-4), 203-226, doi:10.1016/S0169-
1384 7722(02)00204-8, 2003.
- 1385 Lindstrom, G., Johansson, B., Persson, M., Gardelin, M., and Bergstrom, S.: Development
1386 and test of the distributed HBV-96 hydrological model, *J. Hydrol.*, 201, 272-288,
1387 doi:10.1016/S0022-1694(97)00041-3, 1997.
- 1388 Loritz, R., Hassler, S. K., Jackisch, C., Allrogen, N., van Schaik, L., Wienhöfer, J., and
1389 Zehe, E.: Picturing and modeling catchments by representative hillslopes, *Hydrol. Earth*
1390 *Syst. Sci.*, 21, 1225-1249, doi:10.5194/hess-21-1225-2017, 2017.



- 1391 Loritz, R., Gupta, H., Jackisch, C., Westhoff, M., Kleidon, A., Ehret, U., and Zehe, E.: On the
1392 dynamic nature of hydrological similarity, *Hydrol. Earth Syst. Sci.*, 22, 3663-3684,
1393 doi:10.5194/hess-22-3663-2018, 2018.
- 1394 Loritz, R., Kleidon, A., Jackisch, C., Westhoff, M., Ehret, U., Gupta, H., and Zehe, E.: A
1395 topographic index explaining hydrological similarity by accounting for the joint controls of
1396 runoff formation, *Hydrol. Earth Syst. Sci.*, 23, 3807-3821, doi:10.5194/hess-23-3807-2019,
1397 2019.
- 1398 McDonnell, J. J.: The two water worlds hypothesis: Ecohydrological separation of water
1399 between streams and trees?, *Wiley Interdisciplinary Reviews-Water*, 1, 323-329,
1400 doi:10.1002/wat2.1027, 2014.
- 1401 McDonnell, J. J. and Beven, K.: Debates-the future of hydrological sciences: A (common)
1402 path forward? A call to action aimed at understanding velocities, celerities and residence
1403 time distributions of the headwater hydrograph, *Water Resour. Res.*, 50, 5342-5350,
1404 doi:10.1002/2013wr015141, 2014.
- 1405 McGlynn, B. and Seibert, J.: Distributed assessment of contributing area and riparian
1406 buffering along stream networks, *Water Resour. Res.*, 39, WR001521,
1407 doi:10.1029/2002WR001521, 2003.
- 1408 McGlynn, B., McDonnell, J. J., Stewart, M., and Seibert, J.: On the relationships between
1409 catchment scale and streamwater mean residence time, *Hydrol. Proc.*, 17, 175-181,
1410 doi:10.1002/hyp.5085, 2002.
- 1411 McGrath, G. S., Hinz, C., and Sivapalan, M.: Modelling the impact of within-storm variability
1412 of rainfall on the loading of solutes to preferential flow pathways, *Eur. J. Soil Sci.*, 59, 24-
1413 33, doi:10.1111/j.1365-2389.2007.00987.x, 2008.
- 1414 McGrath, G. S., Hinz, C., Sivapalan, M., Dressel, J., Puetz, T., and Vereecken, H.: Identifying
1415 a rainfall event threshold triggering herbicide leaching by preferential flow, *Water Resour.*
1416 *Res.*, 46, W02513, doi:10.1029/2008wr007506, 2010.
- 1417 Milne, G.: Normal erosion as a factor in soil profile development. *Nature*, 138, 548-549,
1418 doi:10.1038/138548c0, 1936.
- 1419 Nash, J. E.: The form of the instantaneous unit hydrograph, *IASH publication no. 45*, 3-4,
1420 114-121, 1957.
- 1421 Niemi, A. J.: Residence time distribution of variable flow processes, *Int. J. Appl. Radiat. Isot.*,
1422 28, 855-860, doi:10.1016/0020-708X(77)90026-6, 1977.
- 1423 Nissan, A. and Berkowitz, B.: Anomalous transport dependence on Péclet number, porous
1424 medium heterogeneity, and a temporally varying velocity field, *Phys. Rev. E*, 99, 033108,
1425 doi:10.1103/PhysRevE.99.033108, 2019.
- 1426 Nissan, A., Dror, I., and Berkowitz, B.: Time-dependent velocity-field controls on anomalous
1427 chemical transport in porous media, *Water Resour. Res.*, 53, 3760-3769,
1428 doi:10.1002/2016WR020143, 2017.
- 1429 Oswald, S., Kinzelbach, W., Greiner, A., and Brix, G.: Observation of flow and transport
1430 processes in artificial porous media via magnetic resonance imaging in three dimensions,
1431 *Geoderma*, 80, 417-429, doi:10.1016/S0016-7061(97)00064-5, 1997.
- 1432 Paik, K. and Kumar, P.: Optimality approaches to describe characteristic fluvial patterns on
1433 landscapes, *Philos. Trans. R. Soc. B-Biol. Sci.*, 365, 1387-1395,
1434 doi:10.1098/rstb.2009.0303, 2010.



- 1435 Paltridge, G. W.: Climate and thermodynamic systems of maximum dissipation, *Nature*, 279,
1436 630-631, doi:10.1038/279630a0, 1979.
- 1437 Refsgaard, J. C. and Storm, B.: MikeShe, in: *Computer models of watershed hydrology*,
1438 edited by: Singh, V. P., Water Resources Publications, Highland Ranch, Colorado, USA,
1439 809-846, 1995.
- 1440 Reinhardt, L., and Ellis, M. A.: The emergence of topographic steady state in a perpetually
1441 dynamic self organised critical landscape, *Water Resour. Res.*, 51, 4986-5003,
1442 doi:10.1002/2014WR016223, 2015.
- 1443 Rinaldo, A., Maritan, A., Colaiori, F., Flammini, A., and Rigon, R.: Thermodynamics of
1444 fractal networks, *Phys. Rev. Lett.*, 76, 3364-3367, doi:10.1103/PhysRevLett.76.3364,
1445 1996.
- 1446 Rinaldo, A., Benettin, P., Harman, C. J., Hrachowitz, M., McGuire, K. J., van der Velde, Y.,
1447 Bertuzzo, E., and Botter, G.: Storage selection functions: A coherent framework for
1448 quantifying how catchments store and release water and solutes, *Water Resour. Res.*, 51,
1449 4840-4847, doi:10.1002/2015wr017273, 2015.
- 1450 Robinson, J. S. and Sivapalan, M.: Catchment-scale runoff generation model by aggregation
1451 and similarity analyses, *Hydrol. Proc.*, 9, 555-574, doi:10.1002/hyp.3360090507, 1995.
- 1452 Rodriguez, N. B., McGuire, K. J., and Klaus, J.: Time-varying storage-water age relationships
1453 in a catchment with a mediterranean climate, *Water Resour. Res.*, 54, 3988-4008,
1454 doi:10.1029/2017wr021964, 2018.
- 1455 Rodriguez, N. B., Pfister, L., Zehe, E., and Klaus, J.: Testing the truncation of travel times
1456 with StorAge Selection functions using deuterium and tritium as tracers. *Hydrology and*
1457 *Earth System Sciences*, submitted, 2019.
- 1458 Rodriguez-Iturbe, I. and Rinaldo, A.: *Fractal river basins: Chance and self-organization*,
1459 Cambridge Univ. Press, Cambridge U. K., 2001.
- 1460 Rodriguez-Iturbe, I., D'Odorico, P., Porporato, A., and Ridolfi, L.: On the spatial and
1461 temporal links between vegetation, climate, and soil moisture, *Water Resour. Res.*, 35,
1462 3709-3722, doi:10.1029/1999wr900255, 1999.
- 1463 Roth, K. and Hammel, K.: Transport of conservative chemical through an unsaturated two-
1464 dimensional Miller-similar medium with steady state flow, *Water Resour. Res.*, 32, 1653-
1465 1663, doi: 10.1029/96WR00756, 1996.
- 1466 Samaniego, L. and Bardossy, A.: Simulation of the impacts of land use/cover and climatic
1467 changes on the runoff characteristics at the mesoscale, *Ecol. Model.*, 196, 45-61,
1468 doi:10.1016/j.ecolmodel.2006.01.005, 2006.
- 1469 Sander, T. and Gerke, H. H.: Modelling field-data of preferential flow in paddy soil induced
1470 by earthworm burrows, *J. Contam Hydrol.*, 104, 126-136,
1471 doi:10.1016/j.jconhyd.2008.11.003, 2009.
- 1472 Savenije, H. H. G.: HESS Opinions "Topography driven conceptual modelling (flex-topo)",
1473 *Hydrol. Earth Syst. Sci.*, 14, 2681-2692, doi:10.5194/hess-14-2681-2010, 2010.
- 1474 Savenije, H. H. G. and Hrachowitz, M.: HESS Opinions "Catchments as meta-organisms - a
1475 new blueprint for hydrological modelling", *Hydrol. Earth Syst. Sci.*, 21, 1107-1116,
1476 doi:10.5194/hess-21-1107-2017, 2017.



- 1477 Scheidegger, A. E.: An evaluation of the accuracy of the diffusivity equation for describing
1478 miscible displacement in porous media, Proc. Theory Fluid Flow Porous Media 2nd Conf.,
1479 101-116, 1959.
- 1480 Scher, H. and Montroll, E. W.: Anomalous transit time dispersion in amorphous solids, Phys.
1481 Rev. B, 12, 2455-2477, doi:10.1103/PhysRevB.12.2455, 1975.
- 1482 Scher, H., Margolin, G., Metzler, R., Klafter, J., and Berkowitz, B.: The dynamical foundation
1483 of fractal stream chemistry: The origin of extremely long retention times, Geophys. Res.
1484 Lett., 29(5), doi:10.1029/2001GL014123, 2002.
- 1485 Sherman, L. K.: Streamflow from rainfall by the unit hydrograph method, Eng. News Record,
1486 180, 501-505, 1932.
- 1487 Simmons, C. S.: A stochastic-convective transport representation of dispersion in one
1488 dimensional porous media systems, Water Resour. Res., 18, 1193-1214,
1489 doi:10.1029/WR018i004p01193, 1982.
- 1490 Šimunek, J., Šejna, M., and van Genuchten, M. T.: Hydrus 2-D software package for
1491 simulating the two-dimensional movement of water, heat, and multiple solutes in variably
1492 saturated media, in, 2.0 ed., U.S. Salinity Laboratory, Agricultural Research Service ARS,
1493 U.S. Department of Agriculture USDA, Riverside, 1999.
- 1494 Šimunek, J., Jarvis, N. J., van Genuchten, M. T., and Gardenas, A.: Review and comparison
1495 of models for describing non-equilibrium and preferential flow and transport in the vadose
1496 zone, J. Hydrol., 272, 14-35, doi:10.1016/S0022-1694(02)00252-4, 2003.
- 1497 Singh, S. K., McMillan, H., Bardossy, A., and Fateh, C.: Nonparametric catchment clustering
1498 using the data depth function, Hydrol. Sci. J.-J. Sci. Hydrol., 61, 2649-2667,
1499 doi:10.1080/02626667.2016.1168927, 2016.
- 1500 Sivapalan, M.: From engineering hydrology to earth system science: Milestones in the
1501 transformation of hydrologic science, Hydrol. Earth Syst. Sci., 22, 1665-1693, doi:
1502 doi:10.5194/hess-22-1665-2018, 2018.
- 1503 Sklash, M. G., and Farvolden, R. N.: The role of groundwater in storm runoff, J. Hydrol., 43,
1504 45-65, doi: 10.1016/0022-1694(79)90164-1, 1979.
- 1505 Sklash, M. G., Beven, K. J., Gilman, K., and Darling, W. G.: Isotope studies of pipeflow at
1506 plynlimon, wales, UK, Hydrol. Proc., 10, 921-944, doi:10.1002/(SICI)1099-
1507 1085(199607)10:7<921::AID-HYP347>3.0.CO;2-B, 1996.
- 1508 Sprenger, M., Tetzlaff, D., Buttle, J., Laudon, H., Leistert, H., Mitchell, C. P. J., Snelgrove, J.,
1509 Weiler, M., and Soulsby, C.: Measuring and modeling stable isotopes of mobile and bulk
1510 soil water, Vadose Zone J., 17, 1-18, doi:10.2136/vzj2017.08.0149, 2018.
- 1511 Sternagel, A., Loritz, R., Wilcke, W., and Zehe, E.: Simulating preferential soil water flow
1512 and tracer transport using the Lagrangian Soil Water and Solute Transport Model, Hydrol.
1513 Earth Syst. Sci. Discuss., doi:10.5194/hess-2019-132, accepted 2019.
- 1514 Tromp-van Meerveld, H. J., and McDonnell, J. J.: Threshold relations in subsurface
1515 stormflow 1. A storm analysis of the Panola hillslope., Water Resour. Res., 42, W02410,
1516 doi:02410.01029/02004WR003778., 2006a.
- 1517 Tromp-van Meerveld, H. J., and McDonnell, J. J.: Threshold relations in subsurface
1518 stormflow: 2. The fill and spill hypothesis, Water Resour. Res., 42, W02411,
1519 doi:10.1029/2004wr003800, 2006b.



- 1520 Turton, D. J., Barnes, D. R., and de Jesus Navar, J.: Old and new water in subsurface flow
1521 from a forest soil block, *J. Environ. Qual.*, 24, 139-146,
1522 doi:10.2134/jeq1995.00472425002400010020x, 1995.
- 1523 van Schaik, L., Palm, J., Klaus, J., Zehe, E., and Schröder, B.: Linking spatial earthworm
1524 distribution to macropore numbers and hydrological effectiveness, *Ecohydrology*, 7, 401-
1525 408, doi:10.1002/eco.1358, 2014.
- 1526 Vogel, H. J. and Roth, K.: Quantitative morphology and network representation of soil pore
1527 structure, *Adv. Water Resour.*, 24, 233-242, doi:10.1016/S0309-1708(00)00055-5, 2001.
- 1528 Vogel, H. J., Cousin, I., Ippisch, O., and Bastian, P.: The dominant role of structure for solute
1529 transport in soil: Experimental evidence and modelling of structure and transport in a field
1530 experiment, *Hydrol. Earth Syst. Sci.*, 10, 495-506, doi:10.5194/hess10-495-2006, 2006.
- 1531 Vrugt, J. A. and Ter Braak, C. J. F.: Dream((d)): An adaptive markov chain monte carlo
1532 simulation algorithm to solve discrete, noncontinuous, and combinatorial posterior
1533 parameter estimation problems, *Hydrol. Earth Syst. Sci.*, 15, 3701-3713, doi:10.5194/hess-
1534 15-3701-2011, 2011.
- 1535 Weiler, M., McGlynn, B. L., McGuire, K. J., and McDonnell, J. J.: How does rainfall become
1536 runoff? A combined tracer and runoff transfer function approach, *Water Resour. Res.*, 39,
1537 1315, doi:10.1029/2003wr002331, 2003.
- 1538 Weinberg, G. M. (1975). *An Introduction to General Systems Thinking*. New York: John
1539 Wiley & Sons, N.Y., p. 279.
- 1540 Westhoff, M. C. and Zehe, E.: Maximum entropy production: Can it be used to constrain
1541 conceptual hydrological models?, *Hydrol. Earth Syst. Sci.*, 17, 3141-3157,
1542 doi:10.5194/hess-17-3141-2013, 2013.
- 1543 Westhoff, M., Kleidon, A., Schymanski, S., Dewals, B., Nijssse, F., Renner, M., Dijkstra, H.,
1544 Ozawa, H., Savenije, H., Dolman, H., Meesters, A., and Zehe, E.: ESD Reviews:
1545 Thermodynamic optimality in Earth sciences. The missing constraints in modeling Earth
1546 system dynamics?, *Earth Syst. Dynam. Discuss.*, doi:10.5194/esd-2019-6, in review, 2019.
- 1547 Wienhoefer, J. and Zehe, E.: Predicting subsurface stormflow response of a forested hillslope
1548 - the role of connected flow paths, *Hydrol. Earth Syst. Sci.*, 18, 121-138, doi:10.5194/hess-
1549 18-121-2014, 2014.
- 1550 Wienhofer, J., Germer, K., Lindenmaier, F., Farber, A., and Zehe, E.: Applied tracers for the
1551 observation of subsurface stormflow at the hillslope scale, *Hydrol. Earth Syst. Sci.*, 13,
1552 1145-1161, doi:10.5194/hess-13-1145-2009, 2009.
- 1553 Wilcke, W., Yasin, S., Valarezo, C., and Zech, W.: Change in water quality during the
1554 passage through a tropical montane rain forest in Ecuador. *Biogeochemistry* 55, 45-72,
1555 doi:10.1023/A:1010631407270, 2001.
- 1556 Worthington, S. R. H. and Ford D. C.: Self-organised permeability in carbonate aquifers,
1557 *Groundwater*, 47(3), 326-336, doi:10.1111/j.1745-6584.2009.00551.x, 2009.
- 1558 Wrede, S., Fenicia, F., Martinez-Carreras, N., Juilleret, J., Hissler, C., Krein, A., Savenije, H.
1559 H. G., Uhlenbrook, S., Kavetski, D., and Pfister, L.: Towards more systematic perceptual
1560 model development: A case study using 3 Luxembourgish catchments, *Hydrol. Proc.*, 29,
1561 2731-2750, doi:10.1002/hyp.10393, 2015.
- 1562 Zehe, E. and Jackisch, C.: A Lagrangian model for soil water dynamics during rainfall-driven
1563 conditions, *Hydrol. Earth Syst. Sci.*, 20, 3511-3526, doi:10.5194/hess-20-3511-2016, 2016.



- 1564 Zehe, E., Blume, T., and Bloschl, G.: The principle of 'maximum energy dissipation': A novel
1565 thermodynamic perspective on rapid water flow in connected soil structures, *Philos. Trans.*
1566 *R. Soc. B-Biol. Sci.*, 365, 1377-1386, doi:10.1098/rstb.2009.0308, 2010.
- 1567 Zehe, E., Ehret, U., Blume, T., Kleidon, A., Scherer, U., and Westhoff, M.: A thermodynamic
1568 approach to link self-organization, preferential flow and rainfall-runoff behaviour, *Hydrol.*
1569 *Earth Syst. Sci.*, 17, 4297-4322, doi:10.5194/hess-17-4297-2013, 2013.
- 1570 Zehe, E., Ehret, U., Pfister, L., Blume, T., Schroder, B., Westhoff, M., Jackisch, C.,
1571 Schymanski, S. J., Weiler, M., Schulz, K., Allroggen, N., Tronicke, J., van Schaik, L.,
1572 Dietrich, P., Scherer, U., Eccard, J., Wulfmeyer, V., and Kleidon, A.: Hess opinions: From
1573 response units to functional units: A thermodynamic reinterpretation of the hru concept to
1574 link spatial organization and functioning of intermediate scale catchments, *Hydrol. Earth*
1575 *Syst. Sci.*, 18, 4635-4655, doi:10.5194/hess-18-4635-2014, 2014.
- 1576 Zehe, E., Loritz, R., Jackisch, C., Westhoff, M., Kleidon, A., Blume, T., Hassler, S. K., and
1577 Savenije, H. H.: Energy states of soil water – a thermodynamic perspective on soil water
1578 dynamics and storage-controlled streamflow generation in different landscapes, *Hydrol.*
1579 *Earth Syst. Sci.*, 23, 971-987, doi:10.5194/hess-23-971-2019, 2019.
- 1580 Zhang, Y., Benson, D. A., and Reeves, D. M.: Time and space nonlocalities underlying
1581 fractional-derivative models: Distinction and review of field applications, *Adv. Water*
1582 *Resour.*, 32, 561-581, doi:10.1016/j.advwatres.2009.01.008, 2009.